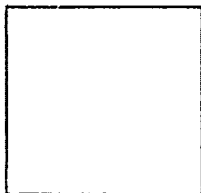


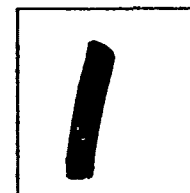
PHOTOGRAPH THIS SHEET

ADA 083532

DTIC ACCESSION NUMBER



LEVEL



INVENTORY

FTD-ID(RS)T-0225-79  
DOCUMENT IDENTIFICATION

DISTRIBUTION STATEMENT A

Approved for public release;  
Distribution Unlimited

DISTRIBUTION STATEMENT

ACCESSION FOR	
NTIS	GRA&I <input checked="" type="checkbox"/>
DTIC	TAB <input type="checkbox"/>
UNANNOUNCED	<input type="checkbox"/>
JUSTIFICATION	
BY	
DISTRIBUTION /	
AVAILABILITY CODES	
DIST	AVAIL AND/OR SPECIAL
A	

DISTRIBUTION STAMP

**DTIC**  
**ELECT**  
**S** APR 24 1980 **D**  
**D**

DATE ACCESSIONED

79      30

DATE RECEIVED IN DTIC

PHOTOGRAPH THIS SHEET AND RETURN TO DTIC-DDA-2

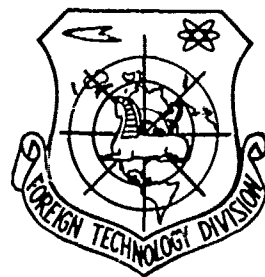
ADA 083532

# FOREIGN TECHNOLOGY DIVISION



STRENGTH OF NONMETALLIC MATERIALS  
DURING NONUNIFORM HEATING  
(SELECTED CHAPTERS)  
by

G. V. Isakhanov



Approved for public release;  
distribution unlimited.



**EDITED TRANSLATION**

FTD-ID(RS)T-0225-79

9 May 1979

MICROFICHE NR: *FTD-79-C-000602*STRENGTH OF NONMETALLIC MATERIALS DURING  
NONUNIFORM HEATING (SELECTED CHAPTERS)

By: G. V. Isakhanov

English pages: 82

Source: Prochnost' Nemetallicheskikh  
Materialov Pri Neravnomernom  
Nagreve, Izd-vo "Naukova Dumka"  
Kiev, 1971, pp. 1-26: 145-178.

Country of origin: USSR

Translated by: SCITRAN  
F33657-78-D-0619

Requester: FTD/TOTA

Approved for public release: distribution unlimited.

THIS TRANSLATION IS A RENDITION OF THE ORIGINAL FOREIGN TEXT WITHOUT ANY ANALYTICAL OR EDITORIAL COMMENT. STATEMENTS OR THEORIES ADVOCATED OR IMPLIED ARE THOSE OF THE SOURCE AND DO NOT NECESSARILY REFLECT THE POSITION OR OPINION OF THE FOREIGN TECHNOLOGY DIVISION.

PREPARED BY:

TRANSLATION DIVISION  
FOREIGN TECHNOLOGY DIVISION  
WP-AFB, OHIO.FTD ID(RS)T-0225-79Date 9 May 1979

TABLE OF CONTENTS

U. S. Board on Geographic Names Transliteration System, Russian and English Trigonometric Functions.....	ii
Summary.....	iii
Introduction.....	iv
Chapter 1. Mechanical Properties of Nonmetallic Materials During Short-Term Heating and Loading.....	1
Chapter 6. Thermal Stability of Refractory Materials..	34
Referenc .....	73
Complete Table of Contents.....	81

U. S. BOARD ON GEOGRAPHIC NAMES TRANSLITERATION SYSTEM

Block	Italic	Transliteration	Block	Italic	Transliteration
А а	<i>А а</i>	A, a	Р р	<i>Р р</i>	R, r
Б б	<i>Б б</i>	B, b	С с	<i>С с</i>	S, s
В в	<i>В в</i>	V, v	Т т	<i>Т т</i>	T, t
Г г	<i>Г г</i>	G, g	У у	<i>У у</i>	U, u
Д д	<i>Д д</i>	D, d	Ф ф	<i>Ф ф</i>	F, f
Е е	<i>Е е</i>	Ye, ye; E, e*	Х х	<i>Х х</i>	Kh, kh
Ж ж	<i>Ж ж</i>	Zh, zh	Ц ц	<i>Ц ц</i>	Ts, ts
З э	<i>З э</i>	Z, z	Ч ч	<i>Ч ч</i>	Ch, ch
И и	<i>И и</i>	I, i	Ш ш	<i>Ш ш</i>	Sh, sh
Й й	<i>Й й</i>	Y, y	Щ щ	<i>Щ щ</i>	Shch, shch
К к	<i>К к</i>	K, k	Ъ ъ	<i>Ъ ъ</i>	"
Л л	<i>Л л</i>	L, l	Ы ы	<i>Ы ы</i>	Y, y
М м	<i>М м</i>	M, m	Ь ь	<i>Ь ь</i>	'
Н н	<i>Н н</i>	N, n	Э э	<i>Э э</i>	E, e
О о	<i>О о</i>	O, o	Ю ю	<i>Ю ю</i>	Yu, yu
П п	<i>П п</i>	P, p	Я я	<i>Я я</i>	Ya, ya

\*ye initially, after vowels, and after ъ, ь; e elsewhere.  
When written as ě in Russian, transliterate as yě or ě.

RUSSIAN AND ENGLISH TRIGONOMETRIC FUNCTIONS

Russian	English	Russian	English	Russian	English
sin	sin	sh	sinh	arc sh	sinh <sup>-1</sup>
cos	cos	ch	cosh	arc ch	cosh <sup>-1</sup>
tg	tan	th	tanh	arc th	tanh <sup>-1</sup>
ctg	cot	cth	coth	arc cth	coth <sup>-1</sup>
sec	sec	sch	sech	arc sch	sech <sup>-1</sup>
cosec	csc	csch	csch	arc csch	csch <sup>-1</sup>

Russian      English

rot      curl  
lg      log

In the monograph problems are considered which are connected with the study of the characteristics of strength and the carrying capacity of nonmetallic materials and structural elements which operate under conditions of a one-sided load and sharp thermal cycling. Original methods and installations are described and results are given from investigation of the strength and carrying capacity of reinforced plastics, devitrified glasses, refractory materials and heat-resistant coatings in the case of nonuniform heating. An analysis is made of the methods of criterial evaluation of heat strength of reinforced plastics in the case of one-sided heating.

The book is intended for scientists and engineering and technical workers who specialize in the area of heat strength.

Responsible editor Academician G. S. Pisarenko, AS, USSR;

Reviewers: Doctor of Technical Sciences G. N. Tret'yachenko and Doctor of Technical Sciences E. S. Ymanskiy.

## INTRODUCTION

The development of new branches of industry, mainly power machinery construction, missile and jet engineering, and aviation is connected with a raising of the operating parameters of parts. Therefore there is an increase in the urgency of investigations of the strength of materials and the carrying capacity of structural elements in a wide range of temperatures (4-4000°K and higher) with different combinations of loads and temperatures; the study of the influence of a vacuum, oxidative and reduction media, radiation, water and combustibles on the mechanical properties of materials.

In recent years there has been an increase in the demand for structural materials with as low a density as possible, possessing high mechanical strength and thermal stability under rigid conditions of force and heat loads. Very promising in this respect are the nonmetallic materials, possessing specific physico-mechanical properties, differing in many respects from the properties of typical metals. Nonmetallic materials, such as reinforced plastics, devitrified glasses, industrial glasses, refractory and other materials are used frequently under conditions in which the traditional metallic materials cannot be used. Thus structures made out of reinforced plastics and metals, under the same conditions of one-sided heating behave differently. Low heat conductivity, high heat capacity and absorption of heat in the case of pyrolysis of the binder predetermine the significantly slowed down heating of reinforced plastic in comparison with metals. This leads to the development, in thin-walled elements, of considerable temperature drops even at low rates of heating. As a result of this constructions made out of reinforced plastics are capable of absorbing considerable force loads with high-temperature short-term heating, while under these same conditions constructions made out of metals lose their working capacity almost completely.

At the present time there is great importance in mechanical tests in the case of intensive one-sided heating and for thermal

resistance, when in a material temperature gradients arise which are regular or irregular in time. A study of the mechanical properties of nonmetallic materials and structural elements made from them in the case of nonuniform heating is possible only on installations which to the maximum degree imitate the real conditions both in the nature and level of force and heat loads and in the conditions of their action. In connection with this, in the initial phase of the investigations the need arose for developing methods of intense heating of the nonmetallic materials and the corresponding test installations. Chapters III and VI of this monograph deal with the description of developed, and those which have been accepted in practice, effective methods of heating by the method of electrical resistance and with the help of radiant energy from a high-temperature emitter on the sample, and other methods, and also of constructions of different heating installations and devices intended for mechanical testing under conditions of intense one-sided heating and sharp heat changes.

Chapters II, IV, V and VI give a description of installations for testing in the case of one-sided heating and some results are given which relate to the heat strength of fiber glasses under conditions of temporary one-sided heating and the heat resistance of refractory materials in the case of sharp heat changes. The results of the investigation of mechanical characteristics given in Chapters V and VI were obtained at the Institute of Strength Problems, AS UkSSR during the last two-three years.

The author expresses his sincere thanks to Academician G. S. Pisarenko, AS USSR for systematic consultation in the preparation of the manuscript, and also thanks to coworkers A. F. Beloivan, V. V. Vengzhen, G. A. Gogots, V. S. Dzyuba, B. A. Lyashenko, V. V. Pasechniy, Yu. M. Rodichev and V. I. Eksin, who took part in the works, the results of which have been used in this book.

Mechanical Properties of Nonmetallic Materials  
during Short-Term Heating and Loading

1. Physical-mechanical properties of structural nonmetallic materials

The requirements of structural materials are quite diverse. It is necessary that such materials, in use, have properties which will ensure the strength and the carrying capacity to support the structural unit at elevated and high temperatures, and under a complex combination of power and thermal effects which change with time and frequently are of a random nature.

In use, one-sided heating or cooling of the piece and sudden one-time or cyclical heat changes are quite prevalent. One-sided heating or cooling takes place on any walls or within partitions which divide the atmosphere into different temperatures - elevated or room, room or low. Other combinations of temperature are also possible, for example during the temperature conditions of pipeline operation for transporting heated or cooled liquids.

One-sided intense aerodynamic heating is used typically for the outer coverings of high speed aircraft and engine housings. During one-sided heating of material, the temperature fields as a rule are nonsteady and nonuniform. The nonsteadiness of the temperature field is determined by the rate of the temperature change  $\frac{dT}{d\tau}$  (where  $\tau$  - time) of the fixed simple volume of the material and absolute value of the highest temperature difference (62).

The nonuniformity of the one dimensional field in the material is characterized by the temperature gradient  $\frac{dT}{dx}$  (where  $x$  - interval), which is the differential characteristic of nonuniformity and temperature drops  $(\Delta T)_{\tau} = T_1 - T_2$  (where  $T_1$  and  $T_2$  - are temperatures of the outer and inner surfaces of the dividing wall material, respectively), and is the integral indicator of nonuniformity. In addition, the temperature field is characterized by a degree of symmetry. In one-sided heating it is asymmetrical relative to the surface, passing across the width of the material.

In general terms we will examine the effect of temperature and load as a function of time on certain mechanical properties of the material and the supporting capacity of the aircraft construction. The operating conditions of the aircraft produce high thermal and power stresses on its most critical parts. Heat flows  $Q$ , acting on certain structures (99) reach 32000 kvt/m<sup>2</sup> or higher (Fig. 1). Aerodynamic heating, accompanying flight at supersonic speeds, greatly increases the temperature of the structural elements.

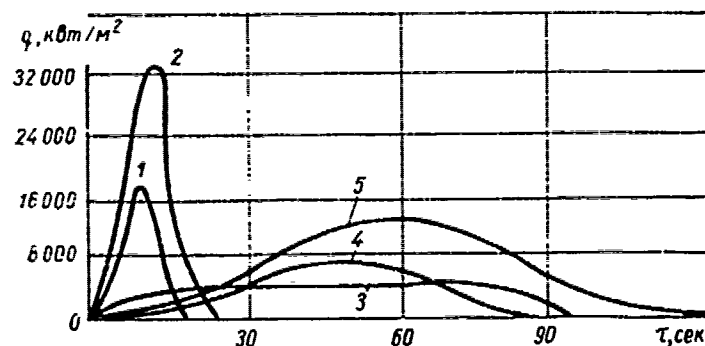


Fig. 1. Typical curves of aerodynamic heating of missiles during entry into dense layers of atmosphere

- 1 - average radius of action ballistic missile;
- 2 - intercontinental ballistic missile;
- 3 - intercontinental gliding missile with jet booster;
- 4 - missile - satellite;
- 5 - superorbital space missile.

Heat exchange is produced by thermal conductivity, convection, and radiation (29, 133). When the air flow at hypersonic speeds is blocked due to obstacles which it encounters, kinetic energy, corresponding to the average speed of air molecules, transforms itself into the energy of the disordered molecule movement, atomic fluctuation, dissociation of diatomic oxygen and nitrogen of the air into monatomic gases with the formation of nitrogen oxide and ionization of gases. Only the first of these phenomena occurs at low supersonic speeds and manifests itself in higher air temperatures. The hot adjoining air layer surrounds the aircraft and heats the structure. When the speed is increased the action of other forms of thermal excitation increases.

1

The temperature of the blocked air layer, i.e. the temperature in the region around the obstacle, where the relative rate of flow is zero, is considerably above 2500°K at Mach number  $M = 8$  (114). At  $M = 20$  (128) the maximum temperature corresponding to the quasi-equilibrium state, is 25000°K. High temperature heating has an adverse effect on the elastic and strength characteristics of structural materials - it lowers the modulus of elasticity, yield strength, and tensile strength. Intense thermal flows, directed inside the structure, due to uneven temperature distribution in the elements, produce widespread temperature gradients, which are the cause of thermal stresses that can exceed material strength and cause losses in stability or failure.

The effect of high temperature is evident also in the fact that even at comparatively low stresses a creep in the material can be observed. Creep deformation due to uneven distribution of stresses and temperature over the separate elements of the structure results in distortion in the shape of the structure. Creep also causes redistribution of stresses in the structure

and losses in stability along the compressed rods. During high temperature heating an intense oxidation occurs which leads to metal failure.

The phenomena described are seen most frequently during long-term thermal loads but can occur also with short-term thermal loads. In supersonic speeds it is necessary also to consider the influence of temperature and time. No one structure is reliable for an unspecified long time period if it becomes heated to an impermissible high temperature. Therefore, it is necessary to protect the supporting metal structure from the direct effects of high temperatures. The effectiveness of the work of the metal-supporting structural parts can be increased by lowering the temperature gradients in it and thus decreasing the intensity of the heat being conducted. At present the inner portions of the structures are protected from excessive overheating by using heat-protecting materials which are applied to the surface of the object to be protected. In sacrificial heat-protecting materials the process of absorption and retardation of the inflowing heat is very complex and includes simultaneous vaporization, sublimation, combustion and carrying off of the cracked and fused material particles (99).

/8 Recently in structures which are subject to high temperature one-sided heating, reinforced plastics (glass-fiber-reinforced materials, asbestos-plastics, carbon-metal-plastics), glass-crystalline materials, heat-resistant commercial glass, oxide refractories and other materials, are used as heat protecting and structural materials for the supporting elements. The nonmetallic materials mentioned have a low thermal conductivity, high heat capacity and several other specific properties. Therefore they can be successfully used in short-term heating of various intensities.

Reference (99) gives information on heat protecting materials of the "Lockheed" grade. These materials can be modified for various systems of heat protection. They are a refractory fiber in an inorganic binder. Due to their diverse density and changeable mechanical characteristics these materials have properties which are not present in homogeneous material. In some cases "Lockheed" can be used both as a heat protecting and as a structural material. The lower layer of "Lockheed" is a supporting base made of high density material and suitable for mechanical fixing to the main structure; this is followed by an intermediate heat insulating layer with low density and a third layer, of a medium density. The type of weaving of the separate layers determines the name of the material. Fig. 2 gives the mechanical properties of "Lockheed" grade materials ( $\sigma$  - tensile strength, E - Young's modulus).

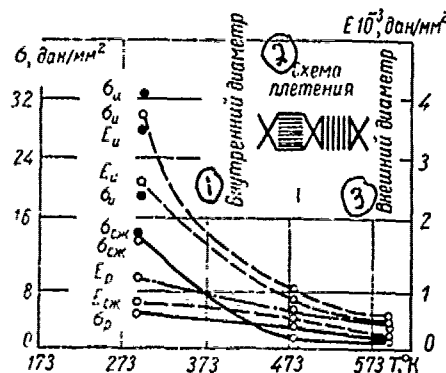


Fig. 2. Mechanical properties of "Lockheed" composition at 293, 473 and 588°K.

○ - transverse bending, cyclic stretching and axial compression;  
● - uniform weaving at 293°K.

Key:

1. Inner diameter
2. Weaving scheme
3. Outer diameter

Commercial glass and setal as well as oxide refractory materials have high heat protecting properties and heat stability during sudden single or multiple heat changes. Oxide refractory materials are used in the form of coating for lining engine combustion chambers, rotating and nozzle turbine blades, antenna devices of aircraft and other pieces, and serve to protect the base material, of which the piece was made, from high temperature, erosion and oxidation effects of the surrounding medium. Such refractory materials are aluminum oxide, magnesium oxide, bilayer coatings, which are combinations of molybdenum disilicide, which is applied directly to the material to be protected, and enamels of various compositions, hafnium oxide or other refractory oxides.

19

Nonmetallic materials, particularly reinforced plastics, are used also as structural material for making the supporting elements of pieces which simultaneously undergo both high strength action and the effects of high temperatures. The behavior of structures, made from glass-fiber-reinforced materials and metals, which have the same geometric sizes and operate under conditions of short term heating, is significantly different. This difference is explained by the characteristics of the thermo-physical properties of the glass-fiber-reinforced plastics. The latter have a high heat inertia due to their low thermal conductivity. The temperature conductivity coefficient of the widely used glass-fiber-reinforced plastic AG-4S is 100 times lower than the temperature conducting coefficient of aluminum or magnesium alloys. The result of this is that even in thin plates or shells made of glass-fiber-reinforced plastics and even at low heating rates considerable temperature drops occur. Under these conditions even in thin metallic plates and shells the temperature redistributes itself evenly across the wall thickness. In glass-fiber-reinforced materials heating

produces structural changes, related to softening, melting, depolymerization and pyrolysis of the binder, as well as the formation of a coke layer on the surface of the material, which causes a softening of the glass-fiber-reinforced material and a worsening of its mechanical properties. The intensity of these processes increases with a rise in temperature and an increase in heating time.

The low thermal conductivity, high heat capacity and heat absorption during pyrolysis of the binder decelerates the penetration of heat inside the wall and prevents a complete heat failure of the material. Because of this glass-fiber-reinforced material, structures maintain a high carrying capacity during nonsteady high intensity heating. The higher the rate and the lower the heating time, the greater the advantages of glass-fiber-reinforced materials in comparison with metals.

The distinctive characteristics of glass-fiber-reinforced materials are their high fatigue limit and corrosion resistance. These materials have a comparatively high strength characteristic per unit weight during tension, compression and bending, high impact resistance, a large reserve strength (at this time only a small portion of the filler strength is realized), making it possible to control the mechanical properties in various directions.

Along with this the use of glass-fiber-reinforced plastics is limited due to their inherent inadequacies. In glass-fiber-reinforced plastics an instability of mechanical properties with time is characteristic. During prolonged heating a sudden worsening of these properties at elevated and high temperatures is observed. The advantage of the glass-fiber-reinforced plastics insofar as fatigue limit is concerned (if temperature and loading times are not considered) in comparison with metals lies mainly during

extension along the fiber (96). Glass-fiber-reinforced plastics have low elongation during tearing, and low tensile strength during shearing along the layers. Notwithstanding the fact that the reinforced glass fibers on the whole increase the rigidity of the filler-matrix composition system, the glass-fiber-reinforced plastics have a low specific rigidity, which limits their use as a structural material for the supporting elements of a part, because low rigidity usually leads to increased weight of the designed structure. The thermal expansion coefficients of glass-fiber-reinforced plastics and metals differ significantly. This makes it difficult to join them or to bond them.

The described disadvantages, as well as the low level of knowledge of the chemical processes of resin ageing, insufficient knowledge of the effect of various loading conditions (power and thermal) on the mechanical properties of these materials has made the designers approach to glass-fiber-reinforced plastics very cautious. However the advantages of glass-fiber-reinforced plastics as a structural material are obvious.

The wide use of inorganic nonmetallic materials as structural materials is limited due to their high brittleness, which remains also at high temperatures, and their sensitivity to the effects of thermal stresses, as a result of which failure occurs at comparatively low temperatures during heating or cooling. The experience accumulated indicates the advantages of using brittle nonmetallic materials in reinforced composition. In this case, obviously, we can expect to obtain materials of lower weight, higher elastic modulus, capable of maintaining strength under conditions of high temperature and sudden heat changes, as compared with metals (70).

## 2. Structural features of reinforced plastics

The structure of reinforced plastics will be examined using glass-fiber-reinforced plastics as the example. The main component parts of glass-fiber-reinforced plastics of any grade are the strengthening (reinforcing) thin fiberglass filler and the binder, a polymeric matrix, selected for their ability to work jointly in the material.

Glass-fiber reinforced plastics are divided into two principle groups dependent on the direction of the fiber: oriented and those with chaotically positioned reinforcement. There is also another classification, forming a separate group of fiberglasses (76). Within these groups five main types of glass-fiber-reinforced materials are found, which are examined, in particular, in reference (104).

As a reinforcing material, fiberglass is used in the form of a coarse linen (a continuous untwisted thread, made up of a large number of strands, each of which has 100-200 fibers), variously woven fabrics, glass mats, made of continuous or staple fibers.

/11

We will examine the structure of a unidirectional glass-fiber-reinforced material. We note that the structural characteristics of the class of composition materials which we are examining are typical of glass-fiber-reinforced plastics, which have different structures, textures or reinforcing plan.

The small diameter glass fibers have an unusually high strength. Thus, a 5-13 micrometer diameter fiber has a rupture strength no less than that of a high quality structural steel. Therefore the most proper structural solution, which will make maximum use of the high mechanical strength of the fibers, is the production of guy unidirectional structures, in which the fiber is arranged in parallel points along the acting tensile forces (116). Unidirectional structures (Fig. 3) can be made on a coarse linen base.

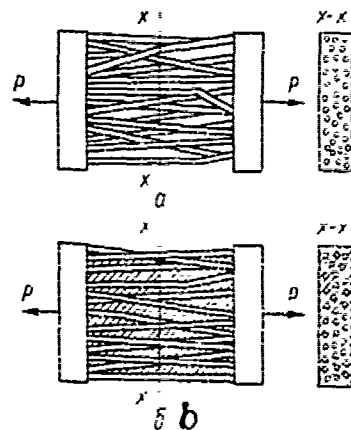


Fig. 3. Phenomenological model of a guy rope structure (a) and glass-fiber-reinforced material (b).

The strength of the unidirectional structures, which are a fibrous mass, is proportional to the content of continuous glass fibers per unit surface of cross section. However, these structures can absorb only tensile stresses. They have very low rigidity, are not capable of maintaining geometric shapes, and are not airtight. Despite the high strength of the initial fibers, their structural strength is not fully realized because the fibers do not all begin to work at the same time and because the strength of the fibers decreases with an increase in their length.

It is obvious that the mass of fibrous material is not yet a commercial material in the generally accepted sense. The strength of the unidirectional structure is considerably increased by glueing the fibers with polymeric binders of various compositions. Actually a new material - glass-fiber-reinforced plastic - is produced only when a binder is added. A polymeric binder, filling all of the empty spaces in a unidirectional structure, transforms it into a compact monolithic medium and gives to it the new properties of a composite material. For example, unidirectional glass-fiber-reinforced plastics are then able, along with tensile forces, to absorb

shear, compressive and bending forces. Thus the fiberglass filler ensures strength and rigidity of the composition system, and the polymeric matrix acts as a binder, redistributing forces among the discrete reinforcing elements, compensating their uneven tension during loading. It makes the material monolithic and ensures its formability. In addition, the binder enveloping the fiber protects it from the effects of the external aggressive medium and mechanical damage, and its chemical-physical properties in considerable measure determine the corresponding properties of the glass-fiber-reinforced plastic.

Due to their structural characteristics glass-fiber-reinforced plastics resist tensile, compressive and bending loads in various ways. The reinforcing fiber is the main supporting force in tension. Therefore the mechanical characteristics of the material in tension are determined mainly by the mechanical properties of the reinforcement, which is almost one or two orders of magnitude above the corresponding mechanical characteristics of the polymeric binder (117).

When reinforced plastics are compressed, the polymeric binding is the strong basic material. Its effect on the mechanical properties of the material is predominant. Also, the reinforcing fibers cemented in the polymeric medium continue to absorb a specified portion of the load, thus improving the tensile strength, elastic modulus and other characteristics of the composition material. However, compression strength and elastic modulus do not attain those values which are observed in glass-fiber-reinforced plastics tension. In particular, the elastic modulus in compression  $E_c$  is lower than in tension  $E_t$  (88, 117). The ratio of moduli  $E_c/E_t$  of various glass-fiber-reinforced plastics fluctuates in the 0.9-0.5 range.

Inasmuch as bending characterizes the inhomogeneity of the stress-strain state, in evaluating the elastic properties of the material it is necessary to take into account the following features: for oriented glass-fiber-reinforced plastics  $E_c \leq E_t$ ,  $E_f \gg E_b$  ( $E_v$  - elastic modulus of fiber,  $E_b$  - elastic modulus of binder). Generally, glass-fiber-reinforced plastics have a layered texture with alternating layers of high module reinforcement and low module polymeric layers (pure or including cross layers of reinforcement). During bending, in addition to normal stresses, tangential stresses appear between texture layers. These cause the polymeric layers to shift. Tangential stresses, in turn contribute to bending deflection due to the effect of so-called texture springiness (68, 101, 102, 103).

The polymeric matrix can redistribute forces in the filler if it has good adhesion to the fiber glass, high cohesion strength and rigidity and deformability which is not lower than the deformability of the glass reinforcement.

13

The binders for glass-fiber-reinforced plastics are a composition of thermosetting or thermoplastic polymeric materials (resin) and solvents. The adhesive substance is the resin. The solvent is used to obtain a binder of specified viscosity, giving the best wettability of the reinforcement.

Five main types of polymeric materials are used as thermo-reactive binders for glass-fiber-reinforced plastics which have the widest application in machinery construction: polyester, epoxy, phenol, melamine, organo-silicon or their various combinations.

Glass-fiber-reinforced plastic is most efficient when it maintains its density as a composite material. Deformability and strength of glass-fiber-reinforced plastic are determined in considerable degree by the combined operation of the glass filler and the polymeric matrix at all stages of the loading system. However, the results of experiment (104, 137) shows that

glass-fiber-reinforced plastics do not always behave as a dense material and the force mechanism in the polymer-glass system depends on how the load is applied, its relative size and how it changes during loading. A theoretical investigation of the density of glass-fiber-reinforced materials was conducted in the work described in reference (138). The model consists of a unidirectional glass core placed in constant tension into a polymer cylinder and enclosed in an elastic body of sufficiently large dimensions. The elastic body was subjected to uniaxial tension along the core axis. It is supposed that the polymer film operates only in shear and the glass fiber only in tension and that both components follow Hooke's Law. The fiberglass forces produce tangential stresses on the surface, which added up across its circumference result in normal forces along the axis of the fiber. Analysis showed that up to the point of shear of the adhesive binder the highest normal stresses act along the center line of the reinforcing fiber and the highest tangential stresses along its ends.

The mechanism of force transmission in the material is determined by the amount of applied load and is not the same at all loading stages. Until shear of the adhesion binder begins, an adhesion mechanism of transmission forces in the glass-fiber-reinforced plastics is observed. However at stresses exceeding the strength of the adhesion binder, in addition to adhesion stresses a friction mechanism of transfer of forces appears which is due to friction forces at the points where adhesion is disturbed. The existence of two mechanisms of force transmission is confirmed experimentally, since in actuality the strength of the glass-fiber-reinforced plastics is at least one order of magnitude or more higher than the strength of the adhesion binder and the strength of the polymeric binder in shear.

/14

One of the deciding factors in forming composition materials is the appropriate selection of components according to mechanical properties,

filler size, and its concentration. For example, if the strength of the binder between the matrix medium and the fiberglass is sufficiently high enough to ensure the same deformation of components under load, then at  $E_v/E_f > 1$  the fiberglass during the process of composition deformation assumes a larger portion of the load, thus lightening the function of the adjoining region of the matrix. The excess load, absorbed by the fiber, is equal to zero at  $E_v = E_f$  and reaches a maximum at  $E_v/E_f = \infty$ .

Fig. 4 shows an idealized stress-strain diagram within the limits of the elastic region for certain real and hypothetical materials (98). The diagram clearly shows that a high elastic modulus of glass fibers in glass-fiber-reinforced materials should make it possible to most effectively utilize their high strength in compositions. This is most obvious if a resin is used in the matrix, for the elastic modulus of the resin is about 20 times lower than the corresponding modulus for glass. Since the resinous matrix can be stretched much further without breaking than fiber, the full strength of the glass filler can be realized in such a composition.

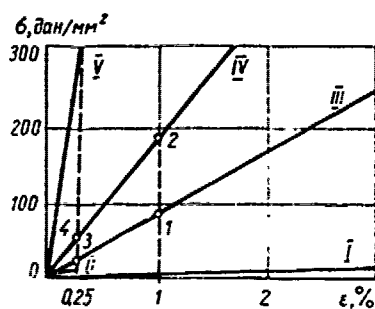


Fig. 4. Elastic region of stress-strain diagram for some real and hypothetical materials at various Young's modulus:

- |                                     |                                      |
|-------------------------------------|--------------------------------------|
| I - $E = 21.7 \text{ ДАТ/мм}^2$ ;   | II - $E = 4600 \text{ ДАТ/мм}^2$ ;   |
| III - $E = 7620 \text{ ДАТ/мм}^2$ ; | IV - $E = 15,050 \text{ ДАТ/мм}^2$ ; |
| V - $E = 76,200 \text{ ДАТ/мм}^2$ . |                                      |

Points 3 and 4 show what stresses can be attained in the inclusions (reinforcement) when the matrix is stretched 0.25%. If a material is selected as the matrix which allows considerable deformation without rupture, then even greater stresses can be attained at these same inclusions (Points 1 and 2).

The length of the glass fiber of the reinforcing filler has an important influence on the strength and the formability of the glass-fiber-reinforced plastics. Fig. 5 compares data on the strength of fiberglass strands with data on the strength of compositions with bases of these strands and epoxy resins in relation to the length of the initial fiberglass (143). As evident from this drawing, the effect of fiberglass length on the strength of the strand and the glass-fiber-reinforced plastic varies. The polymeric matrix in the glass-fiber-reinforced materials increases the strength of the fiberglass strand.

15 The increase in strength of the glass-fiber-reinforced material can be explained from the critical length theory (139). In accordance with the theory for glass-fiber-reinforced plastics the determining factor is not the presence of fine fiber defects but how close they are one to another. According to the degree of loading the fiber breaks at its weakest point, forming shorter and stronger fibers. Breakage continues until the critical length of the fiber is reached, that is the length at which stress in the fiber is equal to the tensile strength and the material breaks. Fracture of highly filled compositions with a high concentration of glass reinforcements has a sharply defined brittle character, while ductile fracture is observed in glass-fiber reinforced plastics which have a low filler content (100).

The presence of adhesion binders between the matrix and the filler and their increased strength results in a decrease in the critical length



high temperatures, adjustments must be made. At higher temperatures the polymeric matrix is weakened which causes a decrease in the strength of the adhesive binder and a lowering of the tangential stresses. The critical length of the fiber is then increased. Under these conditions therefore it is necessary that the length of the fiber be below the critical length at the operating temperatures.

The strength of glass-fiber-reinforced plastics is not a predetermined value. It depends greatly on many factors, particularly on the structure, texture, and the reinforcing plan. The construction technology and the operating factors are also very important.

Glass-fiber-reinforced plastics in which the fibers are arranged chaotically, can, with sufficient accuracy for engineering purposes, be considered quasi-isotropic materials. Their mechanical properties in all directions are approximately the same. In oriented glass-fiber-reinforced plastics the mechanical properties in various directions are different (Fig. 6).

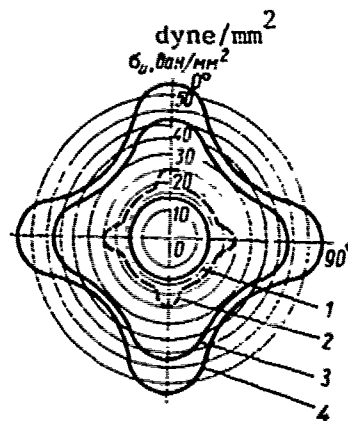


Fig. 6. Relationship of glass-fiber-reinforced plastic bending strength to reinforcement type at various loading angles:

- 1 - mat (short fiber); 2 - laminated filler (mat and fabric);  
 3 - satin woven fabric ( $0 + 90^\circ$ ); 4 - unidirectional fiber ( $0 + 90^\circ$ ).

Such materials are anisotropic, while oriented plastics have a structural anisotropy. The anisotropy of the elastic and strength properties of these

materials is created during the process of their production and is a controlled value. Almost all oriented glass-fiber-reinforced plastics are orthotropic or transversal-isotropic materials (104). Single-directional glass-fiber-reinforced plastics, particularly belong to the transversal-isotropic materials.

### 3. Strength-temperature dependence of reinforced plastics

Temperature is an important factor causing significant changes in the mechanical properties of reinforced plastics. An increase in the temperature affects the strength of the components of these materials in various ways. The reinforcing fiber, in comparison with polymeric, as a rule has much higher mechanical characteristics at elevated and high temperatures. It was determined, for example, that the strength and rigidity of one of the components of glass-fiber-reinforced plastics - fiberglass, is not dependent on temperature in the room-1000°K range (104). It was shown experimentally that the behavior of glass-fiber-reinforced plastics at elevated temperatures depends on the properties and type of the binder, its content, the form of the reinforcement (chaotic reinforcement, fabric, oriented fiberglass) and the method of producing the glass-fiber-reinforced plastic.

17

The effect of temperature on the mechanical properties of glass-fiber-reinforced plastics was described in (22, 24, 28, 49, 53, 78, 85, 89) and so forth. However the results obtained could not be compared because they were obtained on different test stands and by different methods. The comparison is also complicated by the material itself (how it was made, stored and other factors). The investigators established certain general principles of the effect of elevated temperatures on the strength of glass-fiber-reinforced plastics. Thus, an increase in temperature results in chemical-structural changes of the polymeric binder and in a decrease in strength and rigidity of the glass-fiber-reinforced plastics.

It was shown in references (97, 48) that when glass-fiber-reinforced plastics are heated, two contrary processes occur in their binders: the hardening related to structurization concludes and a thermal breakdown occurs. The first process improves the physical-mechanical properties of the material, and the second - greatly impairs them.

The degree and nature of the decrease in strength depend on the duration of the temperature effect and the form of the strength effect (Table 1). The temperature-strength dependence of polymers at temperatures exceeding vitrification temperature (43) is particularly noticeable. Therefore if a glass-fiber-reinforced plastic is to operate successfully at elevated temperatures, it is necessary to select a binder according to its thermal stability.

Following optimal limits of maximum operating temperatures for glass-fiber-reinforced plastics with various binders (75, 148) were experimentally established: for ordinary polyester resins, 350-365°K; for thermally stable polyester resins, to 470°K; for phenol resins, 470-520°K; for epoxy resins, 420-470°K; for organo-silicon resins, to 570°K. It was shown that when the temperature was increased approximately to 310°K, the strength properties of most of the glass-fiber-reinforced plastics with the exception of the one with a PN-1 resin base, did not change. At temperatures above 310°K, the strength properties of glass-fiber-reinforced plastics change in relation to the binder material. Plastics with an epoxy resin (22) base have the highest strength in their initial state; however at 470°K their strength drops sharply in 50-100 hours. Glass-fiber-reinforced plastics on an organo-silicon binder have the lowest strength under ordinary conditions. Also they maintain strength even after 1000 hours of holding at elevated temperatures and this strength remains even

higher than in phenol glass-fiber-reinforced plastics. Fig. 7 shows the effect of temperature on the bending strength of fiberglasses with various binders. The nature of the curves depends exclusively on the thermal stability of the binder.

18

The temperature dependency of strength during tension of oriented AG-4S and 33-18S glass-fiber-reinforced plastics, made with rigid and plastic binders, are shown on Fig. 8 (104).

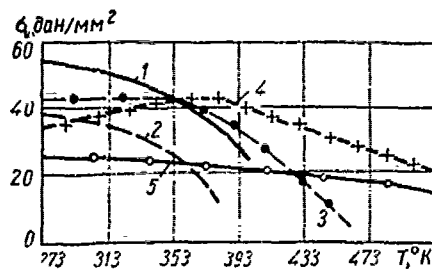


Fig. 7. Relationship of bending strength of fiberglass laminates with different binders to testing temperature:

- 1 - epoxy binder;
- 2 - ordinary polyester binder;
- 3 - heat-resistant polyester binder;
- 4 - heat-resistant phenol binder;
- 5 - organo-silicon binder.

The relative drop in strength  $\sigma_T / \sigma_{293}$ , representing the ratio of strength at testing temperature to strength at room temperature is shown along the ordinate axis. It is seen from this drawing, that materials with a rigid binder have a temperature dependence curve with a greater slope than the curve for materials with a plastic binder.

Table 1. Mechanical properties of various grades of fiberglass  
in relation to heating temperature and time.

Grade of Fiberglass	Testing Conditions		Tensile strength, $\frac{DAT}{\text{mm}^2}$		Elastic modulus upon stretching, $\frac{DAT}{\text{mm}^2}$
	Temperature, $^{\circ}\text{K}$	Time, hrs	Stretching	Bending	
KAST-V	423	5	24,5	—	1127
	473	5	23,5	—	1078
VFT-S	473	0,5	30,0	—	—
	523	0,5	30,8	10,1	1627
	573	0,5	29,8	10,2	1490
	623	0,5	20,5	7,6	1480
EF-32-301	448	200	22,3	8,3	1343
	473	200	21,5	7,1	1146
FN	473	200	23,8	16,7	1303
	523	50	24,2	9,7	1264
	573	10	16,4	11,2	1372
	623	2	12,6	10,5	1274
SK-9F	473	0,5	33,6	15,5	2127
	523	0,5	30,5	14,1	1901
	573	0,5	31,5	12,3	2528
	623	0,5	26,5	12,2	1930
	673	0,5	24,7	11,4	1588
AG-4S glass-fiber-reinforced plastic, equal-strength	423	0,5	11,0	—	1627
	473	0,5	8,9	—	1744
	523	0,5	7,9	—	1225

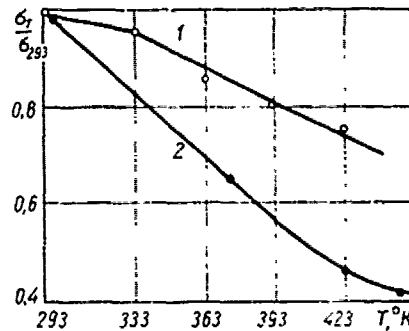


Fig. 8. Temperature dependence of relative strength at extension of oriented glass-fiber-reinforced plastics and various binders:

- 1 - rigid binder (AG-4S);
- 2 - plastic binder (33-18S).

The change in strength as a function of temperature depends on the form of the force effect. In most glass-fiber-reinforced plastics, when the temperature is increased the strength during compression and bending decreases the most. The tensile strength during tension along the fiber decreases at a lesser degree. This is apparently due to the different role of the binder during tension, bending and compression, and changes in the mechanism of force transmission in the material. During bending, when large shear stresses are present which are accepted by the polymeric binder, the strength drop caused by the matrix softening is more perceptible than during tension, when the shear forces are considerably smaller.

During compression when the main force of the glass-fiber-reinforced plastic is the binder (which simultaneously protects the fiberglass from stability loss), the temperature strength dependence is also determined by the thermal stability of the binder.

As a result of the intense decrease in strength during bending, the authors of references (104, 48) consider it advisable to evaluate the efficiency of reinforced plastics during heating according to their bending test results. This is a complex characteristic of the material, which includes the strength of the fiber, the binder and the resistance to shear along the layers.

The resistance of glass-fiber-reinforced plastics to the effects of elevated temperatures is different in various loading directions. This is indicated by the structural anisotropy of the strength properties of the reinforced material. The single-directional glass-fiber-reinforced plastics, loaded in the direction of the reinforcement, have the highest and most stable indicators at elevated temperatures. When oriented glass-fiber-reinforced plastics are loaded at an angle to the axis of the elastic

symmetry, the temperature influence on the strength is greater - the strength is lower, because the working surface of the binder is greater.

Data on the temperature dependence of the mechanical properties of oriented glass-fiber-reinforced plastics and fiberglasses under conditions of elevated temperature (in the 293-573°K) range, are given in reference (24).

/20

Oriented glass-fiber-reinforced plastics (single-directional OSP-10E and those with longitudinal-transverse reinforcement PSP-10E with a 1:1 and 1:2 ratio of layers) are made on an epoxy-phenol binder EFB-4, reinforced with No. 10 glass thread. The binder content was 19-22% by weight, degree of polymerization, 90-95%. The glass-fiber-reinforced plastic was made by winding and then hardening. The fiberglass laminate composition also includes an epoxy-phenol binder, reinforced alkali-free glass fabric ASTT (6) - C<sub>2</sub>. The binder comprises 19-20% by weight, degree of polymerization - 90-95%. The starting data on the mechanical properties of the glass-fiber-reinforced plastics are given in Table 2.

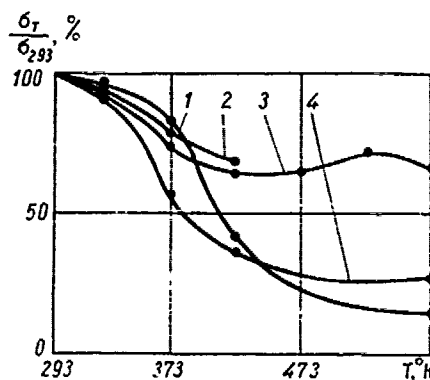


Fig. 9. Relationship of glass-fiber-reinforced plastics relative strength at extension to temperature:

- 1 - fiberglass along woff;
- 2 - unidirectional glass-fiber-reinforced plastic;
- 3 - longitudinal-transverse (1:1) glass-fiber-reinforced plastic;
- 4 - fiberglass along warp.

Table 2. Mechanical properties of glass-fiber-reinforced plastics.

Type of Plastic	$\sigma_B, \text{ n/m}^2 \cdot 10^{-7}$	$\sigma_{\text{comp}}, \text{ n/m}^2 \cdot 10^{-7}$	$E, \text{ n/m}^2 \cdot 10^{-10}$	$\alpha_K, \text{ n/m}^2 \times 10^{-3}$
Unidirectional (1:0)	115*	50.8	4.07	496
Laminated (1:1)				
Longitudinal-transverse	52.4	29.7	2.46	273
Laminated (1:2)				
Longitudinal-transverse	-	36.3	1.92	256
Fiberglass laminate				
warp	46.4	29.3	2.43	-
Fiberglass laminate				
woof	22.9	17.4	1.64	-

\* Tests were made on ring samples 100 mm diameter, 1.0 mm wide and 1.5 mm thick.

To obtain a uniform temperature field, the samples were heated in a heating chamber to the specified level and then held for 15-20 minutes. Test results for standard samples (Fig. 9) show that the temperature during tension of a single-directional glass-fiber-reinforced plastic had a lesser effect on strength, than during tension of a fiberglass laminate. This is also observed in studying the elastic properties. This is not an unexpected conclusion, because in a single-direction glass-fiber-reinforced plastic, the filler has a decisive effect on the strength and elasticity. The filler has a weakly defined temperature dependence on these properties in the examined temperature interval. The test data also show that increasing the

/21

temperature to 373°K sharply decreases the strength of the glass-fiber-reinforced plastics, which differ by structure and filler form. The temperature strength dependence is approximately the same for all glass-fiber-reinforced plastics.

The temperature dependence on the strength of carbon-metal-plastic during tension in uniform heating is shown on Fig. 10. Tests were conducted in an argon atmosphere at 1400°K temperature on a test stand made on a hydraulic machine, TsD-4, base (the test stand was described in Chapter III).

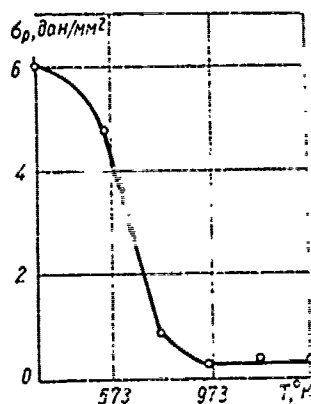


Fig. 10. Temperature-strength dependence of carbon-glass-plastic.

Purity of the inert atmosphere, sufficient for conducting the experiment, was attained by "blowing" the chamber which provided an initial vacuum of  $10^{-2}$  mm Hg and an argon supply. Such "blowing" took place four to five times before each experiment.

Heating was accomplished with a nickel pipe heater. The temperature drop on the working length of the sample, 70 mm, at a maximum test temperature of 1400°K according to five thermocouple readings, did not exceed 5-10 grad. The temperature of the surface of the sample was checked during heating.

When the temperature reached the required value, it was maintained constant until the sample was fully heated. The test stand was equipped with an automatic control device used during heating and holding. The heating rate at all temperature values was a constant 10 grad/sec.

The strength at various temperatures was determined according to data from testing 12-15 samples per point. Fig. 10 shows that generally the strength of the tested plastic decreases (to 80%) at temperatures to 1000°K. A further rise in temperature does not change the strength. A similar temperature-strength dependence of carbon-metal-plastic was observed also in testing for compression and bending.

In evaluating the effect of temperature on the mechanical properties of reinforced plastics, it can be concluded that although a sharp drop in strength occurs in these materials at elevated and high temperatures and uniform heating, due to their thermoconductivities they can be used for short-term operation even at very high temperatures under conditions of one-sided heating.

/22

#### 4. High-temperature strength of glass and sitalls

Data on the temperature strength dependence of inorganic nonmetallic materials is extremely limited. In particular we do not have up to this time such precise information on the temperature dependence of glass as we have, for example, on time dependence. The study of the effect of temperature on the strength of glass is described in references (4, 125, 141, 146). On the basis of an analysis of these investigations in reference (3), an attempt has been made to classify the effect of temperature on the strength of glass.

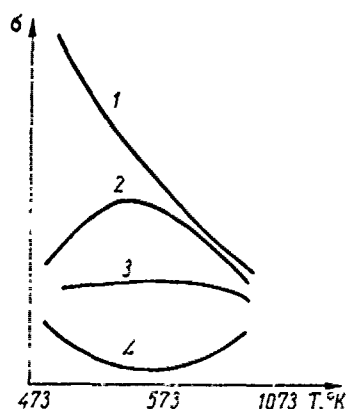


Fig. 11. Four types of silicate glass temperature-strength dependence.

Fig. 11 shows the four types of temperature dependencies of strength of silicate glass. The first type (curve 1) refers to high strength glasses without surface microcracks; the second (curve 2) - to high strength glasses (approximately 100 dat/mm<sup>2</sup>); third and fourth (curves 3 and 4 respectively) - to high strength steels with average (20-30 dat/mm<sup>2</sup>) and with low (5-10 dat/mm<sup>2</sup>) strength.

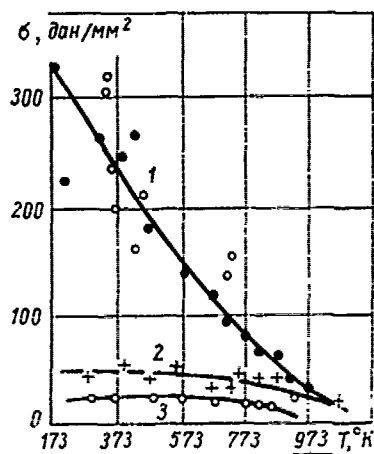


Fig. 12. Temperature-strength dependence of alkali-silicate glass.

As seen from Fig. 12 (curve 1) high strength steels have a sharply dropping temperature dependence (125, 141). The test results were obtained during tensile testing of glass rods, which had been chemically etched and

123

which had a strength of approximately 300 dat/mm<sup>2</sup> at 293°K. The white points correspond to samples 0.3-0.9 mm diameter, and the black points to samples 0.7-1.3 mm diameter. Each point represents 10-20 and above samples tested. Tests conducted by the authors of reference (125) showed a variation coefficient of 4%, and tests conducted by the authors of reference (141) - 5-10%. The sharply dropping temperature dependence of high strength glasses, apparently is produced by the increase in the probability of the formation of microcracks in stressed glass due to the aggressiveness of atmospheric water vapors at high temperatures and the strengthening of the heat motion (fluctuation). It was shown in references (26, 27) that the strength of a defect-free alkali-silicate glass where there is no surface-active medium, decreases with a rise in temperature, but not as sharply as in high strength glass.

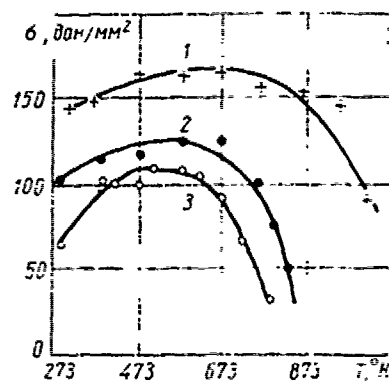


Fig. 13. Temperature-strength dependence of fiberglass during rapid heating:

- 1 - alumoborosilicate fiberglass 11 μm diameter;
- 2 and 3 - alkalisilicate fiberglass 23 μm diameter.

Defective glass fibers, which have a 100-150 dat/mm<sup>2</sup> strength and a 25-30% variation coefficient, are illustrated by curves which have a maximum (curve 2, Fig. 11). Several such temperature dependencies on strength

according to the data of reference (4) are shown on Fig. 13 (curves 1 and 3 were obtained at loading rates of  $3.3 \text{ dat/mm}^2 \cdot \text{min}$ , and curve 2 - at  $300 \text{ dat/mm}^2 \cdot \text{min}$ ). The temperature dependence of low strength glasses with an average strength of  $20\text{-}30 \text{ dat/mm}^2$  is shown in curves 2 and 3 (see Fig. 12). Curve 2 was constructed according to data from reference (141), obtained during rapid extension (several milliseconds) of glass bars  $0.7\text{-}1.3 \text{ mm}$  diameter. Curve 3 was constructed from reference (134) and obtained during tests of strips of  $2.75 \text{ mm}$  thick sheet glass. Fig. 12 shows the drop in strength of these glasses with temperature rise; however this is much weaker than in high strength glasses.

Tests of large glasses showed that the temperature-strength dependence is reflected in curves which have a minimum. In references (145, 146) the drop in strength, in particular, is explained by the fluctuating mechanism of glass breakage, and its increase in strength at high temperatures is due to the fact that surface diffusion rounds off the edges of the microcracks and decreases the stress concentration.

Recently much attention has been given to the synthesis of glass-crystalline materials of a new grade, called sitalls in our literature and known abroad as pyrocerams and glass ceramics. These materials have very valuable properties which make them extremely useful.

/24

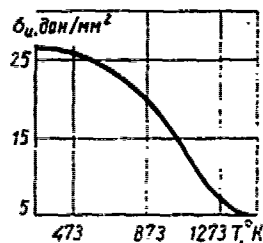


Fig. 14. Effect of temperature on strength of 9606 pyroceramic.

Sitalls are inorganic materials which are obtained by fine crystallization of glasses or melts of various compositions, occurring over the entire volume of a previously shaped piece. Crystallization results in the formation

of an evenly distributed dense microcrystalline structure, characterized by small disordered oriented crystals in the glass phase and the absence of porosity. The size of the crystals ranges from units of micrometers to several micrometers. Microstructural homogeneity ensures the high mechanical properties of the sitalls. Because of their high abrasion resistance in comparison with ordinary glasses, they have a lower sensitivity to those surface injuries which produce stress concentration.

Sitalls are stronger than glass, most ceramic materials and certain metals. When mechanical strength of sitalls is studied, the strength is determined mainly during bending. This method is widely used in testing brittle and difficult-to-work materials, which is mainly due to the simplicity of making the samples and the greater reliability of the average strength values.

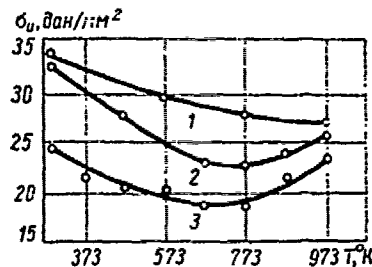


Fig. 15. Effect of temperature on strength of glass-ceramic materials:

- 1 -  $Zr_2O - Al_2O_3 - SiO_2$ ;
- 2 -  $Zr_2O - ZnO - Al_2O_3 - SiO_2$ ;
- 3 -  $Zr_2O - ZnO - SiO_2$ .

It is extremely difficult to determine the strength of brittle materials in tension and in compression. These difficulties are caused by the complex shape of the samples for stretching, and by the concentration of stress appearing at the points where the sample is clamped during tension or on its face surfaces during compression. Inasmuch as sitalls always fail under tensile stress, they cannot be tested for compression because it must be assumed

that at each compression test, failure will occur in the zone of tensile stresses produced by the stress concentrators.

125

Fig. 14 shows the effect of temperature on the mechanical strength of commercial pyroceram 9606 (65). This pyroceram belongs to the category of magnesia-alumosilicate materials. During their production titanium dioxide was used as the catalyst for the formation of crystallization centers. Cordierite is the main crystalline phase in pyroceram. It also contains cristobalite. Strength data refer to rods which have been abrasive-finished and then chemically strengthened. The tensile strength of this material at room temperature is sufficiently high, but with an increase in temperature, its strength drops. However, even at 1073°K the strength of pyroceram considerably exceeds the strength of most glasses at room temperature.

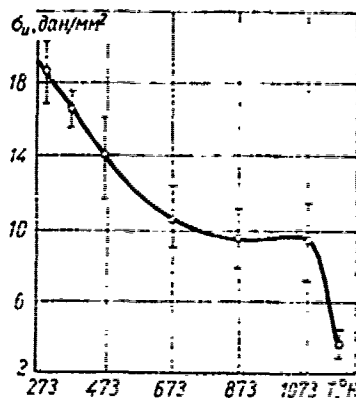


Fig. 15. Strength of sital 123 at temperatures to 1173°K.

In testing glass ceramics of other types, a lowering of strength during heating (curve 1, Fig. 15) is also observed. A similar type of temperature strength dependence during bending for cast sital 123 was determined in reference (118). The results of these studies show that at 1073°K the strength values are less than half of what they are at room temperature.

The authors of reference (118) explain the behavior of the cast sital 123 during heating as follows. Crystallization of light-sensitive glasses

starts from the uniform distribution of centers in the volume of the glass, and a glass phase remains on the outer boundary of each microcrystal. The crystals growing on each center occupy 2-4% less volume than the initial glass. During cooling, as a result of the larger coefficient of linear expansion, the volume of the crystals decreases in greater measure than the volume of the glass. As a result the interlayers of glass between the crystals are in a state of compression, similar to the outer layers of the tempered glass, and the entire system has a high mechanical strength. During heating a reverse reaction occurs and the strength decreases.

A monotonic decrease in strength when temperature rises is also seen in sitall 23. Results shown in Fig. 16 were obtained on prismatic samples measuring 9 x 12 x 80 mm under pure bending conditions after holding them prior to loading for 15 minutes at a test temperature of 1173°K. Curves showing the dependence of strength on temperature were constructed from data on testing 8-10 samples at each point at a mean square error of plus or minus 12%.

In sitalls of some compositions, the initial decrease in strength when temperature rises is followed by recovery of strength at much higher temperatures. This effect is sharply defined for the  $Zi_2O - ZnO - Al_2O_3 - SiO_2$  system (see Fig. 15, curve 2).

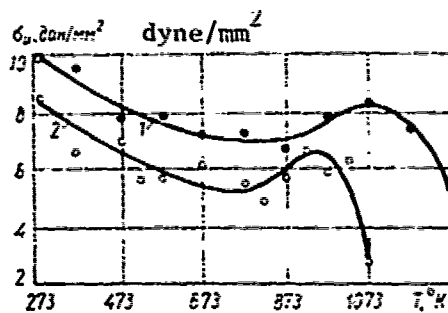


Fig. 17. Temperature-strength dependence of slag-sitalls:

- 1 - slag-sitall495;
- 2 - slag-sitall2.

We obtained the same change in the temperature-strength dependence of slag-sitall 2 and 495 (Fig. 17). The results refer to prismatic samples measuring 9 x 12 x 80 mm. The number of samples per point was 12-15 at a mean square error rate of plus or minus 10%.

Thus, experimental data obtained during uniform heating of brittle nonmetallic inorganic materials indicate that the strength of these materials at elevated temperatures, to 1200-1300°K, greatly decreases, to a point which makes it impractical to use them at these temperatures. But these materials, due to their specific thermal properties, can be successfully used under conditions of short-term, high-temperature, nonuniform heating at temperatures considerably exceeding the above.

## Thermal Stability of Refractory Materials

Materials which are used under conditions of repeated-alternating temperatures must be heat resistant and thermally stable. Thermal stability testing of materials has become very important in recent years. The literature contains a great deal of information on the set-ups and methods used for this purpose (85).

The destructive action of thermal effect is related to the formation of thermal stresses due to temperature gradients, unrestricted heat expansion of the body or its individual zones. Under unfavorable conditions thermal stresses can result in material cracking or its complete failure, losses in the stability of the structural elements and other undesirable consequences. If thermal stability tests for plastic materials are not specific, they are critical for brittle nonmetallic materials and particularly for refractory materials.

Thermal stresses are internal stresses (18, 22, 85), i.e. equalizing within the body itself, its components or a system of several bodies. According to their degree of locality they are divided into stresses of zero, first, second or third order. Thermo-elastic stresses form in an elastic body and disappear after removal of the thermal load: thermo-plastic stresses appear as a result of the transition of a heated body into a plastic state. Sometimes thermal phase stresses appear due to the heterogeneity of the transmission of the nonuniformly heated body into the second phase state.

The test results cited in this chapter represent the thermal stability of materials which are in the brittle state. It is assumed also that the responsibility for failure lies mainly with thermo-elastic stresses of the

first order, i.e. stresses produced by the interaction of a portion of the body with a nonuniform temperature field. The effect of second and third order stresses on thermal stability in this case was not evaluated.

146  
In studying the thermal resistance of materials on simple samples an evaluation is made of the effect of temperature drop and upper temperature of the cycle, degree of sample fastening, prior heat treatment and microstructural stresses, chemical composition, structure and other factors on the number of cycles to thermal fatigue cracking or to the degree of deformation of the sample.

Results obtained on simple samples reflect material properties but do not consider effect on thermal stability of the structural factors which are related to the scale effect and stress concentration. Instead they are initial results inasmuch as a study of thermal stability of pieces should precede a thorough investigation of the thermal stability, mechanical and thermal physical characteristics of the material of which they are made. This is particularly important for a comparative evaluation of the thermal stability of search materials.

In accordance with the systematization presented in reference (85), set-ups for testing thermal resistance of materials using simple-shaped samples and the corresponding test method can be divided into the following groups:

1. Set-ups for testing unfastened samples. In this case the principles of failure are studied and the physical processes of deformation and microstructural changes are mainly determined.

2. Set-ups for testing fastened samples. In these tests thermal stresses which appear as a result of fastening play a very large role. Samples can be fastened to various degrees of rigidity. The accumulation of

cyclical sign-variable plastic deformations results in a change of the shape, dimensions and type of sample failure.

3. Set-ups for testing samples in which the stress state is produced as a result of a nonuniform temperature field. For example, massive cylinders heated and cooled in a gas flow.

Experience has shown that set-ups for testing brittle nonmetallic materials for thermal stability and the corresponding method should make it possible to obtain conditions of thermal loading with temperatures approximately 1500-2000°K and above in a wide range of heating and cooling rates. In order to reduce to a minimum the time during which thermal impact occurs, maximum heating rates at the initial moment (1000 grad/sec and above) are desirable. This can be obtained by so-called inertia-free heating devices. Cooling can be conducted by various media -- still air, compressed inert gas, flowing water or an air-water mixture vortex.

Obviously, requirements as to measurements and registration of process parameters, particularly thermal conditions, temperature levels and field, fixing of the moment of failure, are the same for all test set-ups.

/147

In studying the thermal resistance of brittle nonmetallic materials it is important to efficiently select the shape and sizes of the sample taking into account the specifics of these materials, heating regimes, testing method and so forth. Particularly, in developing the sample it is necessary to provide for small sizes and ease of preparation, and the ability to obtain the desired temperature and stress fields which produce failure under selected conditions of heating and cooling in a comparatively simple manner. Thus, samples of ring and cylindrical shapes which are selected as objects for testing on set-ups, appear to be optimal.

In comparing the thermal regime in testing ring and small cylindrical samples, it should be noted that the regimes for testing the cylindrical

samples are considerably more rigid. Ring samples are tested under quasi-stationary and nonstationary thermal loading regimes, and cylindrical -- under nonstationary regimes.

In testing for thermal impact, thermal stability is expressed by a statistically averaged minimal difference  $\Delta T_{cp}$  between the temperature of the body and the medium during which failure occurs under conditions of a single heat change. In testing for thermal fatigue, thermal stability is expressed by the number  $N$  of multiple heat changes withstood by the samples until failure occurs. Inasmuch as the thermal stability characteristics were conditional to some degree, the results obtained on ring and small cylindrical samples were not compared.

#### 1. Set-ups for testing and small cylindrical samples for thermal stability

The set-up shown on Fig. 97 was designed for testing brittle materials for thermal stability under quasi-stationary and nonstationary thermal loading of the internal surface of the ring samples (19, 21). Heat from the outer surface of the samples is carried away by one of three methods: cooling in the still air zone, during which the surface temperature changes by natural convection, and temperature gradients across the width of the ring are not controlled but are to a considerable degree dependent upon the thermal physical properties of the material; cooling with coolers which contain circulating water, ensuring a large decrease in the temperature of the outer surface due to which quite high temperature gradients can be obtained in the body of sample; cooling in a furnace space with controlled temperature in which case tests can be conducted on specified temperature levels or the temperature of the outer surface can be changed linearly.

/148

The samples used are rings, 25 mm inner diameter, 50 mm outer diameter, 12.5 mm high. The rings are assembled in packets up to 200 mm high, including up to 15 rings.

When the outer surface is cooled using flowing water each of the samples is encircled with detachable copper coolers, 12.5 mm high, comprised of four water-cooled sections. To improve the heat contact of the inner surface each section of the cooler is covered with a layer of soft fusible metal which rubs against the surface of the sample. The sample along with the cooler is placed inside a casing, which is also comprised of four sections. The assembled casings are placed one upon another by special setting recesses and form a packet, which is pulled together with four pins and mounted on the test stand.

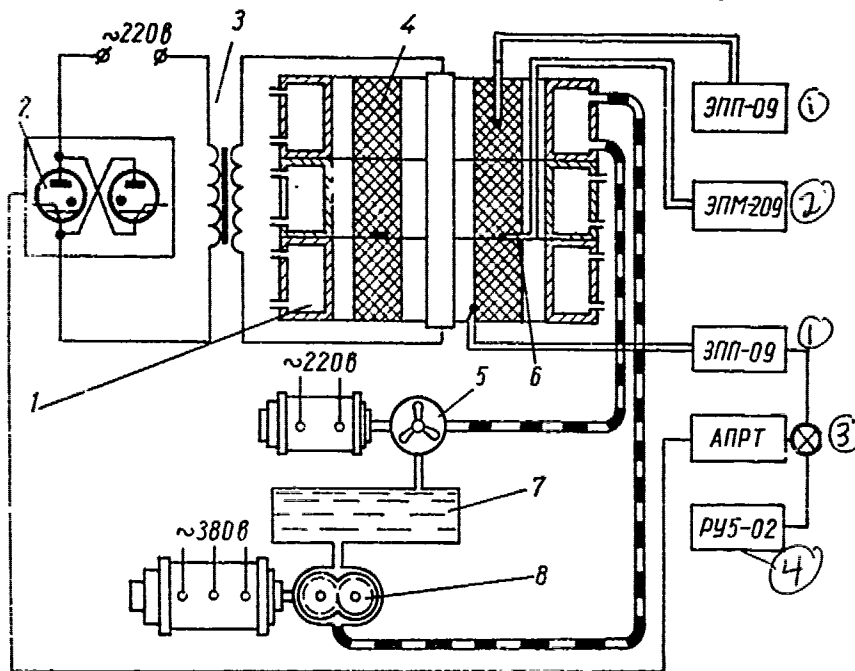


Fig. 97. Schematic of stand for heat resistance testing of ring-shaped samples:

1 - cooler; 2 - switch; 3 - OSU-40 transformer;  
4 - sample; 5 - water pumps; 6 - thermocouple; 7 - water tank.

Key:

1. EPP-09
2. EPM-209
3. APRT
4. RU5-02

The gaps between the rings, which appear in the assembled packet due to the imprecision of sample preparation and the arrangement of thermocouple junctions and thermoelectrodes between the samples, are filled with powder made of a material similar to the material of the sample, dispersed by some kind of an adhesive substance.

/149

The design for fixing the cooler permits the samples to expand in a radial direction and also ensures satisfactory contact between the coolers and samples even in those cases when the samples have been made with engineering imprecision.

Cylindrical rods, made of stainless steels, silicized graphite, silicon carbide or even Silit resistors, are used as heaters. The materials are prepared for use at high temperatures in an oxidizing air atmosphere. Heaters 8-23.5 mm diameter are fastened in water cooled clamps. The heaters are long enough, 250-320 mm, so that the flow of heat from their cooling ends does not disturb the uniformity of temperature distribution in the heating zone.

Test results are considerably affected by the degree of accuracy of the coaxial position of the heating element inside the packet of samples. To avoid uneven heating of the samples the heaters are centered using coordinate devices. The use of coordinate devices makes it possible to conduct the tests when the heater and the samples are misaligned, for the coordinates can adjust the misalignment.

The heating system allows the temperature to be increased on the inner surface of the sample at a rate from 1-2 to 500 grad/min. Two systems of single phase transformers are used: a regulating transformer ROT-25 with a power transformer OSY-40 and a voltage regulator RNO-10 with a furnace transformer PT-7. This makes it possible to vary the heating rate and in

combination with the cooling rate conduct testing under regimes, which in a relatively large range, model the natural conditions of the work of the material in the piece.

The test set-up is equipped with an automatic system of heat control, shown in Fig. 9<sup>o</sup> (20). The system uses an ignitron contactor IK, suitable both for switching the electric supply on and off, and for maintaining even control of power to the heater.

The contactor is assembled on counter-parallel connected metal ignitrons type I-140 (0.8). The power through the ignitron into the heater can be changed by symmetrically changing the ignition angles. The contactor is controlled using an automatically programmed temperature regulator APRT. A rheostat temperature gauge 15, which has a 100% proportional band, is placed on the one-second potentiometer EPP-09M5 on one axis with a main slide rheostat. The heating program employs an automatic device RJ5-02M based on the principle of automatic tracing a program applied on a diagram tape. The driving potentiometer 13 is connected to the photo tracing system so that a signal, proportional to the current value of the temperature specified by the heating program, can be recorded at the outlet of the programming device. The temperature sensing rheostat 15 and the driving potentiometer 13 are connected by a bridge schematic fed from the stabilized voltage supply 14.

/150

The continuous control heating system ensures smooth regulation of the temperature on the surface of the samples both at small (approximately 1 grad/min), and at large (approximately 500 grad/min) rates of increase. The advantage of this system is that it makes it possible to reproduce thermal loading regimes with high precision.

The development of techniques which make it possible to register the failure of the sample is very important in testing for thermal stability.

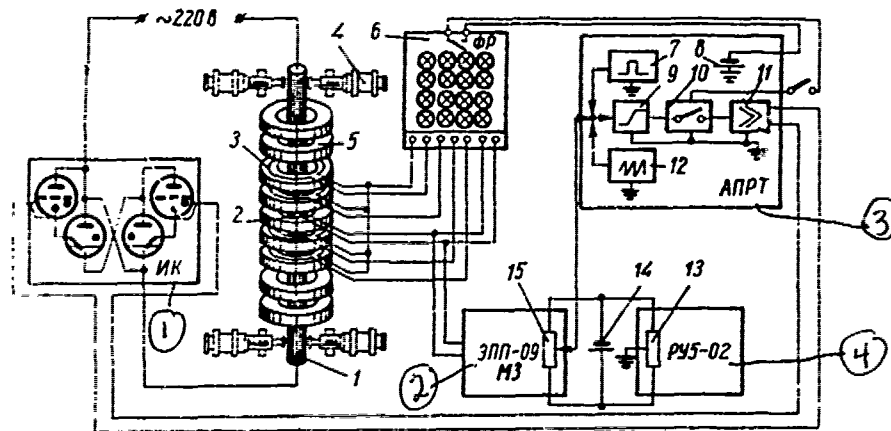


Fig. 98. Block-schematic of automatically controlled heating system:

- 1 - heater; 2 - temperature gauge; 3 - rupture gauge;  
 4 - coordinator; 5 - sample;  
 6 - device for fixing the breaking moment; 7 - power governor;  
 8 - current source; 9 - phase displacer;  
 10 - electronic bridge; 11 - power amplifier;  
 12 - sawtooth voltage generator; 13 - driving potentiometer;  
 14 - stabilized voltage supply; 15 - temperature sensing rheostat.

Key:

1. ИК  
 2. ЕРР-09 МЗ  
 3. АРРТ  
 4. РУ5-02

The test set-up has a special device (21) which fixes the moment and the order of failure when it receives the appropriate signal from the sample. A current-conducting compound with electrodes soldered to it is applied to the ends or side surfaces of the sample, as a failure gauge.

The moment of failure is registered by a method described in reference (21). A block-schematic of the device for fixing the failure moment is shown in Fig. 99. When the sample and its gauge fail, an electrical impulse on its sensor 2 appears in the block of the unit signal 1. The impulse is directed to the executing block 4 and storage block 6. When the executing block receives

the impulse it immediately closes the circuit of temperature gauge 3, as a result of which the amount of electromotive force at the outlet of instrument 5 (EPP-09 potentiometer) decreases to zero, which is noted in the form of a splash (dash) on the temperature line recorded by this instrument. In this way the amount of failure of each sample is recorded.

Because the impulses obtained by the executing block 4 during failure of any sample from the packet are the same, in order to establish the order of sample failure, storage block 6 serves to fix the sequence of the impulses from the unit signal 1 blocks. By comparing these recordings on instrument 3 and the data from storage block 6, the moment of failure of each sample can be determined. The registration system is low-inertial and permits a precise determination of the moment of actual failure.

Samples of other sizes can also be tested on this test set-up, for example, samples 30/25 mm diameter, but over 12.5 mm high. In these cases (when testing in coolers) several coolers are used simultaneously.

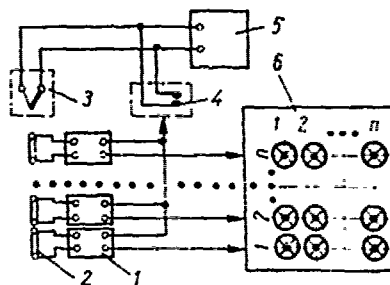


Fig. 99. Block-schematic of device for fixing the sample breaking moment.

Small cylindrical samples are tested in two ways: when testing for thermal impact, an intensive single heating is used with subsequent cooling; when testing for thermal fatigue of materials, cyclical, multiple alternating heat changes (heating - cooling) are used.

The establishment of the failure regimes in testing small cylindrical samples for thermal stability is very difficult inasmuch as materials such as the refractory materials have high brittleness and low thermal conductivity. They fail only when there is a large increase in heating and cooling rates. Regimes with high heating rates can be obtained using inertia-free elliptical heating devices, and cooling - air-water mixture vortexes.

A block-schematic of the test set-up which provides the failure regime during testing of small cylindrical samples is shown in Fig. 100 (120, 121). Samples are heated by focused radiant energy from a heating device which consists of an elliptical cylinder closed at the ends. A schematic of the heating device is shown in Fig. 101. The optimal design-engineering problems in developing similar devices and the feasibility of using these devices are examined in Chapter III.

152

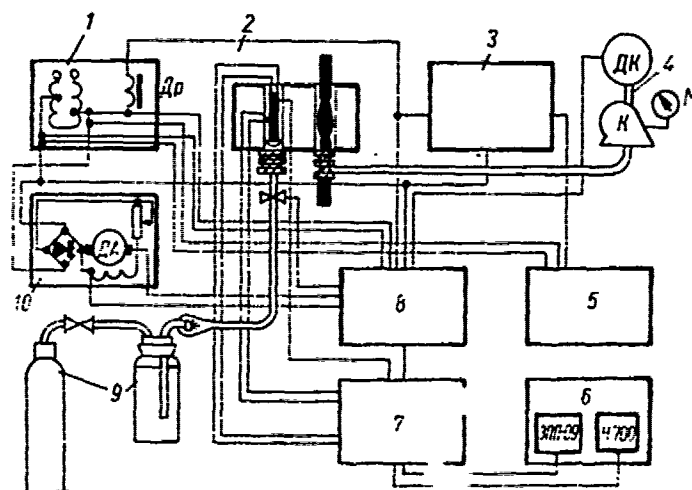


Fig. 100. Block-schematic of installation for heat resistance testing of small samples:

- 1 - power supply unit; 2 - sample heating block;
- 3 - high-voltage pulse generator; 4 - arc stabilizer;
- 5 - signalling unit;
- 6 - temperature control and thermoelectromotive force recording unit;
- 7 - sample rotating and fixing, emf output system;
- 8 - electric relay control unit; 9 - sample cooling unit;
- 10 - automatic angle feeding unit.

The large semi-axis of the ellipse used on this stand measures 67 mm, and the small - 45 mm. The interfocal distance is 51 mm, the height is 20 mm. At 110 v and 40 amp current intensity the heating device, made of polished copper, allows temperatures to 2000°K in 4-6 seconds at an initial heating rate of 500-600 grad/sec and above on the surface of a cylindrical sample of some approved materials measuring 5 mm diameter, 20 mm high.

At higher power inputs the temperature ceiling is 2300-2500°K. So, for example, at 40 v voltage and 150<sup>amp</sup> current intensity, a temperature of 2300°K is obtained in 5-8 sec on a sample of the same dimensions, made of aluminum oxide. If a silvered screen is used, then due to the much higher integral reflecting capacity of silver, the specified temperature can be obtained without increasing the power input.

153 The air-water mixture under pressure from a compressor is passed through a vortex generator and uniformly cools the surface of the sample being tested. Oscillographs have shown that a constant temperature of the cooling atmosphere, equal to 330-340°K, is established in 0.3-0.5 sec, i.e. almost instantaneously. The compressor rating is 120 watts and the highest allowable pressure in the accumulator is 3.2 atm. Its productivity is 22 l/min at 2.2 atm pressure. Under such heating and cooling conditions samples, which were 4-7 mm diameter and 18-20 mm high cylinders, conditionally designated as small, were brought to failure during tests for thermal fatigue and thermal impact.

The electrical system of the test set-up (Fig. 102) under single and multiple thermal loading conditions provides for carbon arc ignition and maintaining its electrical parameters, switching in the system for heating the sample and simultaneously switching in a system for cooling by an air-water mixture, subsequent heating of the sample and so forth.

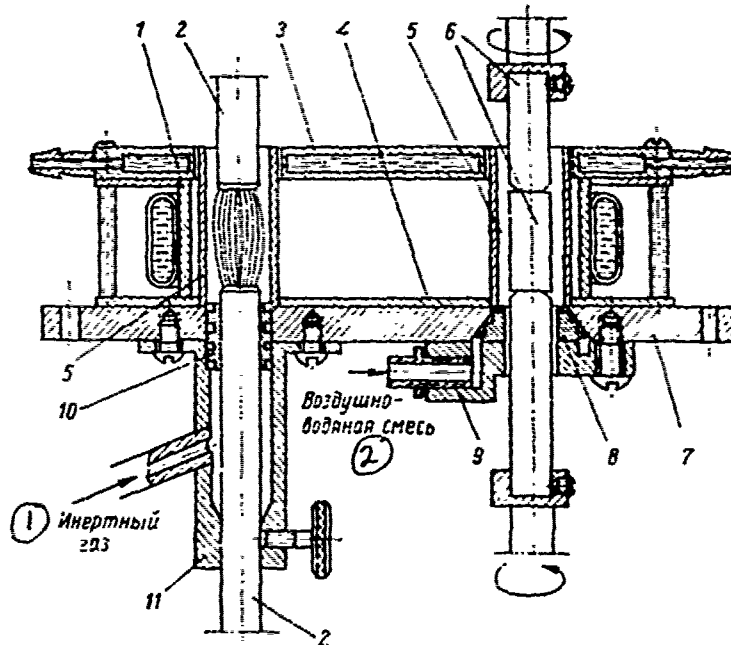


Fig. 101. Heating unit in installation for heat-resistance testing of small samples:

- 1 - heater housing; 2 - electrodes; 3 - upper cover;
- 4 - lower cover; 5 - quartz tubes; 6 - sample with clamps;
- 7 - mounting plate; 8 - vortex generator;
- 9 - vortex generator housing;
- 10 - vortex generator for arc stabilizer;
- 11 - electrode holder case.

Key:

- 1. Inert gas
- 2. Air-water mixture

The test cycle is begun by pushing button  $P_1$ , whereupon the magnetic starter K coil is switched on, which closes the normally open contacts 1K (interlocking button  $P_1$ ), 3K and 4K. Voltage is supplied to the compressor motor DK, and compressor K begins to operate. In addition, the normally open contact 2K closes, preventing the possibility of switching on the electrical arc when there is no sample being cooled by the vortex of air-water mixture.

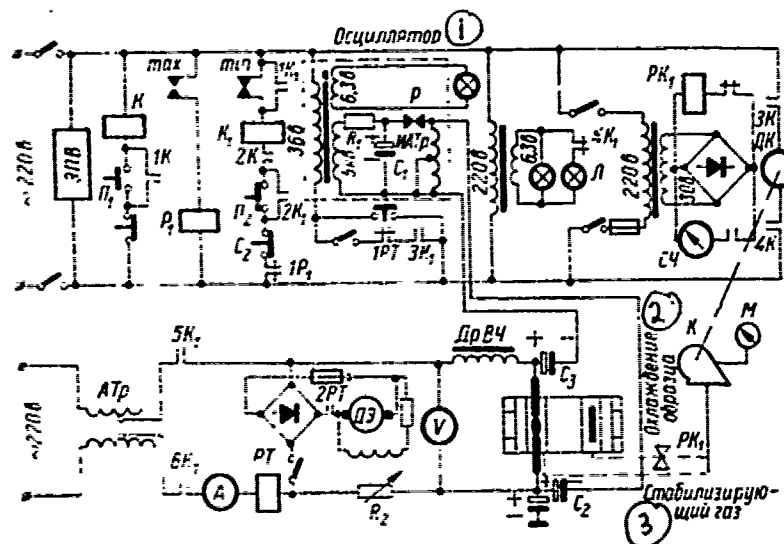


Fig. 102. Electrical schematic of installation.

Key:

1. Oscillator
2. Sample cooling
3. Stabilizing gas

Heating is switched on with button P<sub>2</sub>. If contacts min on EPP-09 are closed, then voltage is supplied on the magnetic starter K<sub>1</sub> winding. The normally open 1K<sub>1</sub> and 2K<sub>1</sub> contacts of starter K<sub>1</sub> interlock the corresponding min contacts and P<sub>2</sub> button and take the starter to self-feeding. The normally 5K<sub>1</sub> and 6K<sub>1</sub> contacts close and through them the operating arc voltage is supplied onto the electrodes from the voltage regulator ATP type RHO-250-10. This is signalled by light bulb L, which goes out when contact 4K<sub>1</sub> is closed.

Contacts 3K<sub>1</sub> switch on the step-up transformer which supplies the high voltage pulse generator. Voltage up to 5KV at 50 hertz frequency is supplied from the secondary winding of the step-up transformer through resistor R<sub>1</sub>, equal to 15 kom, on the oscillatory circuit, comprised of capacitor C<sub>1</sub>

type KSO-13 (0.2 microfarad, operating voltage 5KV), spark arrester P and inductance in the form of a primary winding pulse autotransformer IAT<sub>1</sub>. Voltage to 30 KV at 300-500 kilohertz frequency, necessary for electrical circuit breakdown, forms at the outlet of the autotransformer. The autotransformer is mounted on ferrite cores. The high voltage pulse ionizes the air in the gap between electrodes and provides for carbon arc ignition. Under working conditions the current relay RT type ET-523/6 operates. By normally closed contacts 1PT, it switches on the high voltage pulse generator and by normally open contacts 2PT, switches on the motor of the mechanism for moving the electrodes DE.

The voltage regulator AT<sub>p</sub> of the arc supply circuit is protected from high voltage by the high frequency choke DrVCh, placed in an oil bath. The choke is made on a ferrite core and is connected sequentially in the regulator circuit. High voltage from the secondary winding of the pulse autotransformer IAT<sub>p</sub> is fed to the electrode through separating capacitors C<sub>2</sub> and C<sub>3</sub> (0.4 microfarad, operating voltage 1KV). The choke and capacitors C<sub>2</sub> and C<sub>3</sub> serve to partially separate the circuit of high voltage and the operating arc voltage.

The voltage conducted to the electrodes is regulated from 0 to 250 v. The operating arc voltage is controlled by volt meter V, and the operating current - ammeter A. Reading of heating and cooling times is fixed by an electric stopwatch. So that the arc will burn steadily, a balanced resistor R<sub>2</sub> is sequentially connected into the circuit. A "dropping" volt-ampere characteristic is thus obtained.

The electric arc burns on high intensity grade "Extra-affect" 7-8 mm diameter carbon films. The arc is placed coaxially in a 15.5 mm diameter quartz tube. Argon, which stabilizes the carbon arc, is supplied along

the axis of the electrodes from top to bottom across spiral channels of the vortex generator at 2-3 atm pressure. The vortex generator is a ring 10 mm high and 15.4 mm diameter which has spiral channels with a 1.5 mm pitch at an angle of  $25^\circ$  to the cylindrical surface of the ring notched on the periphery. The channel cross section is 2 x 2 mm.

The test stand is equipped with a mechanism which automatically maintains a constant gap between the electrodes. The electric motor of the mechanism is supplied through a rectifier assembled by a bridge scheme on type D304 diodes, from AT<sub>p</sub> voltage regulator. The voltage supply taken from AT<sub>p</sub> regulator changes from 0 to 40 v in relation to the required feed rate of the upper electrode.

Automatic temperature changes in the specified range are made by the min and max contact of the one-second EPP-09 potentiometer from platinum-platinum-rhodium thermocouples 0.1 mm diameter. When the maximum temperature is reached, the max contacts close P<sub>1</sub> relay, which instantaneously closes the normally open 1P<sub>1</sub> contact and connects the magnetic starter K<sub>1</sub>. The heating circuit is disconnected and the min contacts are unlocked by the normally open 1K<sub>1</sub> contact. The normally open 3K and 4K contacts are disconnected, the magnetic valve PK<sub>1</sub> operates and connects the air cooling of the sample by the air-water mixture vortex. When the minimum temperature is reached the voltage is supplied to the magnetic starter K<sub>1</sub> and the cycle repeats itself.

156

The test stand has an attachment for fixing and rotating the sample to equalize the temperature on its outer surface (Fig. 103). The attachment consists of an upper moveable support and a lower fixed support in the vertical direction. Sample 3 is placed on the supports and using a fixing rod 6, it is entered into the region of focus of the elliptical cylinder 1. The sample is correctly placed in the cylinder plane with the help of a scale applied to the fixing rod.

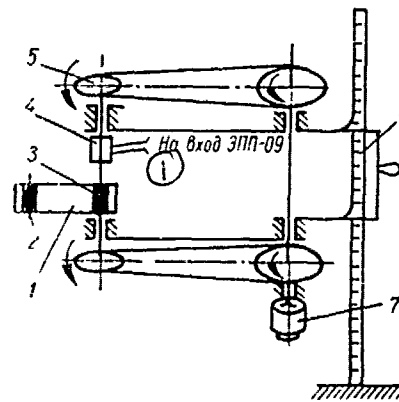


Fig. 103. Schematic of attachment for fastening and rotating sample.

Key:

1. At entrance to EPP-09.

When the arc 2 is connected the sample begins its rotary movement by means of electric motor 7 and four pulleys 5. The thermocouple electrodes are brought out on current collector 4. Temperature equalization on the outer surface of the sample is attained by experimentally selecting its rotation rate, which is determined by the changes in the temperature rate during heating and cooling.

The sample temperature on its outer surface, core and at intermediate points is measured by platinum-platinum-rhodium thermocouples 0.1-0.2 mm diameter. The thermoelectromotive force from the thermocouples goes to a specially constructed current collector comprised of a collection of small diameter copper pulleys placed at specified intervals or an insulating sleeve which is rigidly located on the roller which rotates with the sample. The thermoelectromotive force which goes to the copper pulleys is removed by silver-plated sliding chords and fed to the EPP-09 electron potentiometer at a carriage speed of 1 sec. The current collector, as the experiment revealed, is highly reliable.

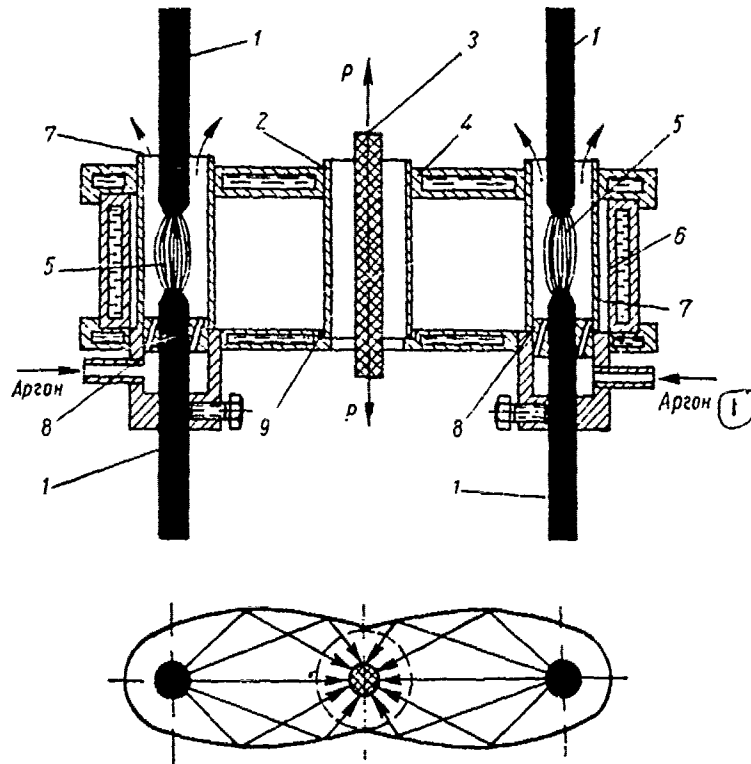


Fig. 104. Schematic and cross-section of two-lobe heating device:

- 1 - carbon electrodes; 2,7 - quartz tubes; 3 - sample;
- 4 - water-jacketed upper lid; 5 - arcs;
- 6 - water-jacketed elliptical reflector;
- 8 - vortex generators;
- 9 - water-jacketed bottom lid.

Key:

- 1. Argon

Thus the test set-up makes it possible to automatically regulate the maximum temperature of the cycle, heating and cooling rate, temperature interval of the cycle, automatically drop the sample to cool it in water, fix the working position of the sample, ensuring maximum reproducibility of the test results. The test set-up provides for testing in a controlled atmosphere. In this case the sample is placed in a quartz tube filled with a specified medium.

/157

Unlike the single-lobe heating device examined above whose disadvantage is the nonuniformity of temperature distribution on the outer surface of the sample, a two-lobe device, due to the symmetrical arrangement of the heating radiator in relation to the sample, provides for uniform heating. A schematic and cross-section of the two-lobe heating device are shown in Fig. 104. The main structural elements of this device are two reflectors (lobe) which are shaped like closed elliptical cylinders with a common focal axis. A high temperature radiation heating source (39) is located along the second focal axis of each reflector.

The two-lobe heaters provide for various programs of thermal action on the sample being tested. If necessary they can be used for each radiation source separately.

/158

## 2. Thermal stability of ring and small cylindrical samples

Ring samples were tested on a test stand described in section 1 of this chapter (19, 21). The thermal stability of refractories obtained by greatly differing methods was studied, as well as their structure, chemical composition, and mechanical properties. Samples of aluminum oxide containing titanium oxide and commercial aluminum oxide were prepared by casting from dross. Commercial aluminum oxide, various compositions of aluminosilicates, magnesial concrete on a phosphate binder and other materials were used to prepare samples by pressing. Hereon for the sake of brevity the samples will be divided into cast and pressed.

The cast refractories were produced in the experimental plant of the Ukrainian Scientific Research Institute for Refractories in accordance with technical specifications MRTU-14-06-25-65. The pressed refractories were search materials of the Materials Engineering Institute, Academy of Sciences Uk SSR.

Table 8. Porosity and density of refractories.

Material	Porosity, %	Density, kg/m <sup>3</sup> · 10 <sup>2</sup>
Al <sub>2</sub> O <sub>3</sub> + TiO <sub>2</sub>	0-5.0	3.65
Al <sub>2</sub> O <sub>3</sub> (cast)	0-5.0	3.7
Al <sub>2</sub> O <sub>3</sub> (pressed)	29.8	2.66
ZrO <sub>2</sub>	26.1	3.99
Dense magnesian concrete	19	-
Porous magnesian concrete	35	-
Alumosilicates (0-10% EN)	8-12	-
Alumosilicates (20-70% EN)	20-40	-

To obtain the most reliable experimental data, the samples were carefully sorted and graded before testing. To reduce the effect of engineering factors on the test results to a minimum, samples were made from the same raw material in one batch, i.e. they were produced under the same heat treating conditions.

The samples were selected according to external appearance, color, weight and size. The variations of weight and size did not fluctuate more than plus or minus 0.75% and plus or minus 0.25 mm, respectively, as an average for the batch (21).

Some information on the samples and the materials from which they were made are shown in Tables 8-11. Fig. 105 shows the temperature dependence of the modulus of elasticity and Poisson's coefficient for aluminum oxide containing titanium and pressed aluminum oxide. Typically, when temperature

Table 9. Chemical composition of refractories (%).

Material	Al <sub>2</sub> O <sub>3</sub>	ZrO <sub>2</sub>	SiO <sub>2</sub>	TiO <sub>2</sub>	Fe <sub>2</sub> O <sub>3</sub>	MgO	CaO
Al <sub>2</sub> O <sub>3</sub> + TiO <sub>2</sub>	98.92	-	0.09	0.9	0.05	0.02	0.01
Al <sub>2</sub> O <sub>3</sub> (cast)	99.73	-	0.1	0.01	0.08	0.05	0.01
Al <sub>2</sub> O <sub>3</sub> (pressed)	99.37	-	0.24	-	0.13	-	-
ZrO <sub>2</sub>	1.09	90	1.4	1.16	1.16	-	6.46

Table 10. Dimensions of refractory ring samples.

Material	Outer diameter, mm	Inner diameter, mm	Height, mm
Al <sub>2</sub> O <sub>3</sub> + TiO <sub>2</sub> (first batch)	49	24.8	13.6
Al <sub>2</sub> O <sub>3</sub> + TiO <sub>2</sub> (second batch)	49.5	24.9	13.7
Al <sub>2</sub> O <sub>3</sub> + TiO <sub>2</sub> (third batch)	39.8	17.7	12.2
Al <sub>2</sub> O <sub>3</sub> (cast, first batch)	50.3	25.4	14.0
Al <sub>2</sub> O <sub>3</sub> (cast, second batch)	49.6	24.8	13.8
Al <sub>2</sub> O <sub>3</sub> (pressed)	50.1	24.3	51.3
Al <sub>2</sub> O <sub>3</sub> (pressed)	50.2	24.3	52.5
ZrO <sub>2</sub>	51.8	24.4	50.4
Dense magnesian concrete	49.6	25.8	48.0
Porous magnesian concrete	49.9	25.5	51.1
Uncalcinable magnesian concrete	50.5	25.2	12.6
Alumosilicates (0-10% NE)	51.1	26.2	12.0
Alumosilicates (20-70% NE)	50.4	25.2	12.2
Red brick	50.1	24.9	12.5

rises to 1100-1400°K, the elastic modulus and Poisson's coefficient and the linear expansion coefficient of the specified materials changes very slightly. This makes it possible to compare the test results obtained for these materials at various temperatures with a sufficient degree of accuracy without further correction.

Table 11. Bending strength ( $\text{kg}/\text{cm}^2$ ) of refractories.

Material	Temperature, °C				
	20°	473	573	773	973
$\text{Al}_2\text{O}_3 + \text{TiO}_2$	79.0	78.0	76.5	-	74.0
$\text{Al}_2\text{O}_3$ (pressed)	14.2	19.2	-	16.2	-
Alumosilicate (5% NE)	18.5	-	-	-	-
Alumosilicate (50% NE)	4.9	-	-	-	-

The method provides for testing under quasi-stationary (stationary) and nonstationary thermal loading conditions. Quasi-stationary (stationary) heating conditions are obtained by slowly (at a rate not higher than 2  $\text{grad}/\text{min}$ ) but continuously increasing the internal surface temperature of the sample or by gradually (at 25-50  $\text{va}$ ) increasing the electric current supplied to the heater. It is apparent by comparing both heating methods, that the first method provides more uniform and stable testing conditions. This makes it possible to very simply determine temperature changes in the sample and to compare data corresponding to failure at various times with high accuracy.

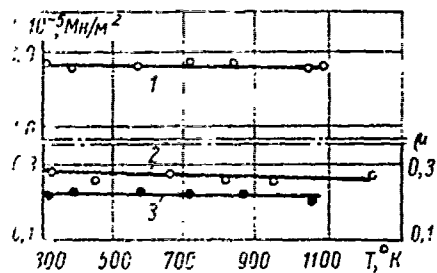


Fig. 105. Temperature dependence of elastic modulus  $\underline{E}$  and Poisson's coefficient  $\alpha$ :

- 1 - elastic modulus  $\text{Al}_2\text{O}_3 + \text{TiO}_2$ ;
- 2 - elastic modulus  $\text{Al}_2\text{O}_3$  (pressed);
- 3 - Poisson's coefficient.

Nonstationary conditions are maintained by a constant electrical power (1-8 kva) supplied to the heater, or a constant rate (50-500 grad/min) of heating of the inner surface of the sample (21). The sample is cooled with flowing water or air.

A platinum-platinum-rhodium thermocouple, 0.1-0.5 mm diameter, is used to measure heat and determine the distribution of temperature across the thickness of the ring. Thermocouples are placed in four-six points along the radius of the ring at the end or directly on the side surface of the sample, to which a thin layer of cement of a specified composition has been applied. The cement may also have been applied in special recesses made for this purpose into which the thermocouples were soldered. Experience showed that the thermocouples were best fastened to the sample by soldering.

The thermoelectromotive force of the thermocouples was measured and registered by single-point electron automatic self-recording potentiometers EPP-9, M3 grade 0.5.

The failure moment was fixed by a special device described in paragraph one of this chapter. The failure gauge is a thin layer of material in the form of a narrow strip which is applied to the sample surface. The sample is considered to have failed when the continuity of such a gauge has been disturbed. All the experimental data are averaged values obtained on the basis of testing 10-12 samples (21).

161

Testing under quasi-stationary conditions revealed the resistance of the refractory material to slowly increasing thermal loads, which corresponded to stationary loading conditions. The results obtained are shown in Table 12. The temperature distribution across the thickness of the pressed aluminum oxide samples is shown in Fig. 106a. Table 12 shows that the thermal stability characteristics are greatly affected by the outer surface sample cooling conditions.

Table 12. Thermal stability of ring samples during quasi-stationary heating.

Material	Inner and outer diameters of samples, mm	Breaking temperature gradient, grad		
		$\Delta T_{\text{min}}$	$\Delta T_{\text{av}}$	$\Delta T_{\text{max}}$
Al <sub>2</sub> O <sub>3</sub> + TiO <sub>2</sub>	49.0/24.8	75	98	115
Al <sub>2</sub> O <sub>3</sub> + TiO <sub>2</sub>	49.0/24.8	75	88	121
Al <sub>2</sub> O <sub>3</sub> (pressed)	50.1/24.3	133	172	211
Al <sub>2</sub> O <sub>3</sub> (cast)	50.3/25.4	68	82	99
Al <sub>2</sub> O <sub>3</sub> (cast)	49.6/24.8	71	103	125
Alumosilicate (0% NE)	51.1/26.2	145	175	207
Alumosilicate (5% NE)	51.1/26.2	308	317	331
Dense magnesia concrete	49.6/25.8	78	114	140
Porous magnesia concrete	49.9/25.8	170	227	270
Uncalcinable magnesia concrete	50.5/26.2	150	231	265
ZrO <sub>2</sub>	51.8/24.4	65	92	117
Red brick	50.1/24.9	39	47	76
Alumosilicates (20-70% NE)	50.4/25.2	Did not break at $\Delta T_{\text{aver}} = 920$ grad		

A comparison of the effect of various coolers on the thermal stability of samples made from aluminum oxide plus titanium oxide showed that when their outer surface was cooled in the still air zone (first line) the outer surface temperature, at 1003°K, corresponded to the average failing temperature drop, 98°. When the outer surface temperature was cooled in coolers with flowing water (second line) at a temperature drop of 88 grad, the temperature of the outer surface was 403°K. A decrease in the amount of failing temperature gradient when cooling conditions were intensified was observed in other materials also. For example, samples from cast aluminum oxide, cooled in the still air zone failed at an average temperature gradient of approximately 155 grad (outer surface temperature was 1048°K), and those cooled in the cooler at 148 grad (outer surface temperature 523°K). A decrease in the failing average temperature gradient due to an increase in cooling intensity was noted particularly in the work described in (144).

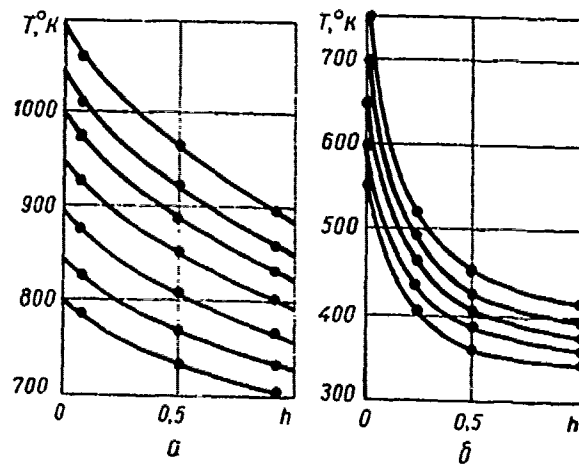


Fig. 106. Temperature distribution through pressed aluminum oxide sample upon quasi-stationary heating at 2 grad/min (a) and nonstationary heating at 340 grad/min (b).

Analyses of temperature distribution across the thickness of the ring under various outer surface conditions indicates that distribution is not the same when different coolers are used. When cooling in the zone closest to the surface being cooled is more intensive, a larger relative temperature drop is noted. This apparently is due to the effect of the boundary conditions of heat exchange, which determine the temperature distribution in any nonsteady process including a quasi-stationary one, which can be regarded as a process with a weakly defined nonsteadiness.

It may be concluded that in quasi-stationary conditions, for a more complete evaluation of thermal loading resistance it is necessary to consider the actual temperature distribution producing sample failure along with the degree of the falling temperature gradient. In comparing the thermal stability of materials it is necessary to apply criteria which take into account the thermal state of the samples being tested.

153

Tests in nonsteady thermal loading conditions showed the effect of the temperature change rate on the thermal stability of the samples and also the efficiency of the materials under these heating conditions. The thermal energy was supplied at a constant electrical current power and constant increase in temperature on the outer surface of the samples. Apparently the higher heating rates result in very rapid changes in the temperature field and predetermine much higher values of temperature gradients. Fig. 106b shows temperature distribution in samples in nonstationary heating.

Tables 13 and 14 show test results for thermal stability in relation to heating conditions. Experimental data on the thermal stability of aluminum oxide containing titanium oxide obtained at various but constant heating rates of the internal surface of the samples, are shown in Table 13.

Table 13. Thermal stability of ring samples in aluminum oxide with titanium oxide admixture during nonstationary heating.

Sample size (inner and outer diameters) mm	Heating rate, grad/min	Breaking temperature gradient		
		$\Delta T_{\min}$	$\Delta T_{\text{aver}}$	$\Delta T_{\max}$
49.0/24.8	50	88	101.5	112
	170	118	123.4	131
	340	136	141.8	155
39.8/17.7	170	103	112	125
	34	133	140	158

Table 14. Thermal stability of ring samples under various thermal loading conditions.

Material	Heater capacity or temperature change rate	Breaking temperature gradient		
		$\Delta T_{\min}$	$\Delta T_{\text{aver}}$	$\Delta T_{\max}$
Al <sub>2</sub> O <sub>3</sub> (pressed)	170 grad/min	214	229	234
	340 grad/min	284	297	305
	2000 volt-amp*	330	342	355
	3000 volt-amp*	323	374	448
Al <sub>2</sub> O <sub>3</sub> (cast)	50 grad/min	83	102	122
	175 grad/min	109	116	117
	7 kva* (400 grad/min)	118	182	270

\* Thermo-couples were soldered to sample surface.

/16L

It should be noted that when the heating rate is increased, the value of the temperature gradient at which failure occurs increases. A similar increase in the failing gradient is observed when the thermal load intensity is increased for samples of other materials also (Table 14).

The thermal stability of aluminum silicate was determined at various constant increases of temperature on the inner surface of the ring. Test results are shown in Fig. 107. For comparison, data are shown which were obtained during heating when the electrical power was maintained at a constant rate. The data refer to the average heating rate on the inner surface of the samples. A comparison of the results indicates that the relationship between the values of the failing temperature gradients of each composition under different thermal loading conditions is approximately the same, if the

samples are heated at a constant rate. An analysis permits us to draw the very important conclusion that for an approximated comparative evaluation of the thermal stability of materials it is more advisable to test them under rapidly occurring heating conditions than under slow quasi-stationary conditions. In the first case along with greatly shortened testing times it is possible to obtain higher temperature gradients in the samples and therefore investigate the thermal resistance of a larger number of materials.

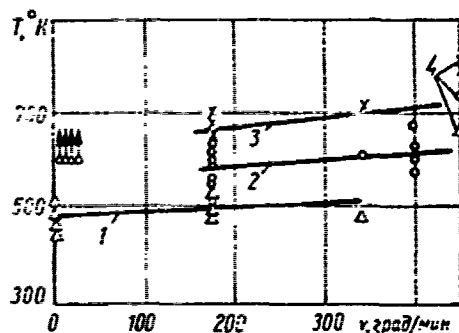


Fig. 107. Thermal stability of aluminosilicate samples containing various amounts of boron nitride:

- 1 - NB = 0%;
- 2 - NB = 5%;
- 3 - NB = 10%;
- 4 - heating with constant electrical capacity  $\bar{N} = 3$  kva heaters.

Fig. 108 shows test data on aluminosilicate compositions. The effect of the amount of boron nitride content on thermal stability was determined according to the failing temperature difference at the same temperature heating rate on the outer surface of the samples. Boron nitride content was 0.5; 7 and 10%. As is shown, an increase in the amount of boron nitride at a selected heating rate of 170  $\text{град/мин}$ , results in an increase in the failing temperature gradient.

The nature of the failure of refractories obtained by casting and pressing differs (21). Samples made from materials obtained by casting failed very

quickly and failure is accompanied by a characteristic snapping sound. In most cases only a radial crack appears. The crack is located as a rule at the point of a defect. Some samples at failure divide into two portions, and at higher heating intensities parts of the sample fly in various directions, and the failure process itself resembles an explosion.

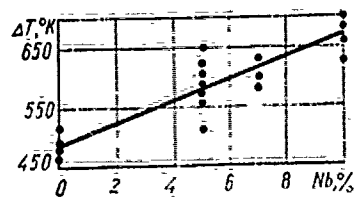


Fig. 108. Effect of boron nitride on heat resistance of samples during nonstationary heating at 170 grad/min.

Pressed samples fail gradually. The crack forms on one end of the sample and as the temperature gradient increases the crack spreads, with many pauses, in the axial direction. Almost always after the first crack forms, after a certain time other cracks follow. Study of crack microsections and fracture characteristics has shown that the staggered or skipping character of fracture is due in considerable measure to material porosity. The cracks appear in the most weakened sections where there are the largest accumulations of pores or other internal defects. They stop in the larger round pores which contribute to thermal stress drop. When the stress level rises, as a result of the increase in the temperature gradient, the crack again begins to spread to new rounded pores where it becomes sequentially localized.

Small cylindrical samples, 4-8 mm diameter and 18-20 mm high, were tested in nonstationary heating and cooling conditions on the test set-up which was described in paragraph of this chapter. The following refractory materials were tested for thermal impact and thermal fatigue: special porcelain, porcelain, starting glass and glass-based citall, aluminum oxide containing 1% titanium oxide, produced by casting. Silicon carbide, aluminum oxide,

magnesium oxide and calcium zirconate, made by powder metallurgy, were also tested. (The chemical composition and physical-mechanical properties of most of these materials are given in Tables 15 and 16).

When the materials were tested for thermal impact, that is in a single heat change, the failing difference was determined by gradually increasing the sample temperature while maintaining the rate, density and temperature (330-340°) of the cooling air-water mixture. Initially the thermal stability limits were determined by approximation. Samples were tested, for example, at 1300-1600°K. If it appeared that samples did not fail at temperatures below 1300°K and failed at 1600°K, then it was not necessary to test them at temperatures above 1600°K and below 1300°K. Later the temperature interval was measured every 50 grad and thus the value of the failing temperature difference was established. To test correctly for thermal stability approximately ten results per point are necessary; however because test results for small samples do not have a wide scatter, the number of tests per point can be reduced to five or seven.

/156

Table 15. Chemical composition of refractories, wt %.

Starting materials	SiO <sub>2</sub>	Al <sub>2</sub> O <sub>3</sub>	Fe <sub>2</sub> O <sub>3</sub>	CaO	MgO	K <sub>2</sub> O	Na <sub>2</sub> O	ZnO	TiO <sub>2</sub>	AlFe
Porcelain	55.0	34.48	0.54	1.24	0.26	1.73 (in total)	-	0.62	-	-
Special porcelain	4.0	45.0	0.48	1.11	0.25	1.4 (in total)	0.3	11.46	-	-
Starting sital glass	60.0	16.0	-	-	15.5	1.5	1.0	-	-	6.0

Note: Data obtained in Institute of Silicate Chemistry, USSR Academy of Sciences.

Table 16. Physico-mechanical properties of refractories.

Parameters	Material			
	Starting siall glass	Siall	Porcelain	Special porcelain
Density, $\text{kg/m}^3$	$2.5 \cdot 10^{-3}$	$2.61 \cdot 10^{-3}$	=	=
Young's modulus, $\text{data/mm}^2$	$7.3 \cdot 10^3$	$6.7 \cdot 10^3$	=	=
Shear modulus, $\text{data/mm}^2$	306	369	$8.4 \cdot 10^3$ 334	$10 \cdot 10^3$ 388
Poisson's coefficient, $\frac{\text{data/mm}}{\text{mm}^2}$	0.213	0.216	0.26	0.28
Bending strength, $\text{data/mm}^2$	5.9	30.6	=	=
Compression strength, $\text{data/mm}^2$	51	122	=	=
Linear expansion coefficient at 273-573°K, 1/grad	$78.5 \cdot 10^{-7}$	$63.8 \cdot 10^{-7}$	$3.3 \cdot 10^{-6}$	$2.9 \cdot 10^{-6}$
Impact viscosity $\frac{\text{data/mm}}{\text{mm}^3}$	$1.8 \cdot 10^{-2}$	$4.5 \cdot 10^{-2}$		

Note: Data obtained in Institute of Silicate Chemistry,  
USSR Academy of Sciences.

Samples which did not fail during impact tests can be later used at the same temperature differences for thermal fatigue testing. Fatigue is determined by the number of cycles of specified heat changes which the sample withstands until failure. The heating-cooling cycle is the same as that used in testing for thermal impact.

Temperatures in the core or in the intermediate points between the core and the surface are measured with a platinum-platinum-rhodium thermocouple 0.1-0.2 mm diameter, the junction of which is placed in an 0.5 mm diameter opening and fused with silver. A good bond was thus achieved between the thermocouple junction and the sample material. The surface temperature of the sample was also measured by a thermocouple, the junction of which was tied with a zirconium thread. The thermoelectrodes were insulated with alundum capillaries. Each sample was carefully examined before testing and

Table 17. Thermal stability of small cylindrical samples.

Material	$\Delta T_{aver}$	$\alpha^*$	$\alpha^*$	$\alpha^*$	Test temperature range, K
		1 vt/m <sup>2</sup> grad	2 vt/m <sup>2</sup> grad	3 vt/m <sup>2</sup> grad	
Al <sub>2</sub> O <sub>3</sub>	1235	=	318	=	1573-338
MgO	1155	=	318	=	1473-338
SiC	1285	=	318	=	1623-338
Al <sub>2</sub> O <sub>3</sub> + 1% TiO <sub>2</sub>	635	=	=	720	973-338
Special porcelain	1280	222	=	=	1618-338
Special porcelain	1140	=	=	720	1478-338
Porcelain	750	222	=	=	1098-338
Porcelain	700	=	318	=	1038-338
Porcelain	615	=	=	720	953-338
Starting sitall; glass	535	=	318	=	873-338
Setal	655	=	318	=	993-338

after each heat change. Failure was fixed according to appearance of cracks detected under a microscope.

Small samples were tested for thermal stability under thermal impact and thermal fatigue conditions at the following heat exchange coefficients:

$\alpha_1^* \approx 222$ ,  $\alpha_2^* \approx 318$  and  $\alpha_3^* \approx 720$  vt/m<sup>2</sup> x grad (119). The results obtained in testing materials under heat impact conditions are shown in Table 17 in which  $\Delta T_{av}$  designates the failing temperature difference.

Analysis of the obtained results show that of the materials investigated those most resistant to thermal impact are aluminum oxide, magnesium oxide, silicon carbide, special porcelain and aluminum oxide plus titanium oxide. The failing temperature difference for these materials was in the 1150-1300°K range.

A steady decrease in resistance at thermal impact was observed when the heat exchange coefficient,  $\alpha^*$ , was increased. Thus, for special porcelain a change in heat exchange coefficient from 222 to 720 vt/m<sup>2</sup> • grad produced a decrease in temperature failing difference of 140 grad. A similar tendency was

determined also for porcelain which was tested at heat exchange coefficients of  $\alpha^* = 222, 318$  and  $720 \text{ vt/m}^2 \cdot \text{grad}$ . The drop in the failing temperature difference in relation to the value of the failing temperature difference at  $\alpha^* = 222 \text{ vt/m}^2 \cdot \text{gradient}$  was 50 and 135 grad. In all cases the temperature of the air-water cooling mixture was constant and approximately  $338^\circ\text{K}$ . Apparently the tendency to the drop in thermal resistance when the heat exchange coefficient was increased was general.

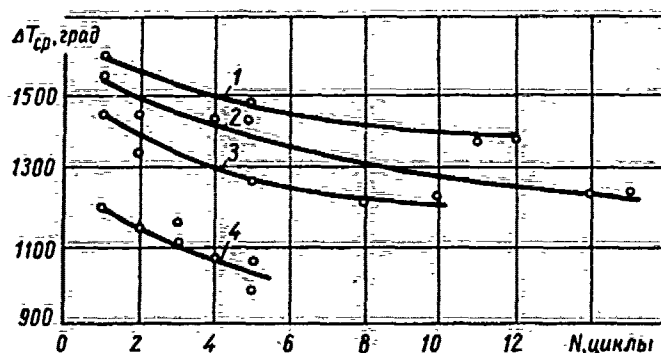


Fig. 109. Relationship of thermal stability to number of cycles to breakage at heat exchange coefficient  $\alpha^* = 318 \text{ vt/m}^2 \cdot \text{grad}$ :

- 1 - silicon carbide;
- 2 - aluminum oxide;
- 3 - magnesium oxide;
- 4 - porcelain

The great difference in the values of failing temperature differences for porcelain and special porcelain is explained by the effect on thermal resistance of such factors as the method of producing the material, the grain size of the initial structural component (special porcelain has a finer grained structure), sample size (the porcelain sample diameter was 5.5 mm and the special porcelain - 4 mm). When the sample diameter was lower under otherwise equal conditions, the value of the failing temperature difference increased. For example, tests of porcelain at  $\alpha^* 318 \text{ vt/m}^2 \cdot \text{grad}$  showed that the failing temperature difference with a sample diameter decrease (7; 4.5 and 4 mm) increased at an average by 40%.

Fig. 109 gives test results for thermal fatigue of pressed silicon carbide, aluminum oxide, magnesium oxide and cast porcelain at a constant heat exchange coefficient  $\alpha^* = 318 \text{ wt/m}^2 \cdot \text{grad}$ . The failure of samples in most cases was observed both along the generatrix as well as perpendicular to it.

### 3. Thermal Stability and Heat protecting Properties of Some Nonmetallic Coatings

159 The necessity for protecting structural materials from the destructive effect of an aggressive (oxidizing) atmosphere led to the development of possible heat resistant protective coatings, which affect the strength and efficiency of the base material both as a result of the process by which they were applied as well as by the physical-mechanical properties of the coatings. The criterion of the effectiveness of the heat protecting coatings applied is their maintenance of mechanical properties stability in the protected structural materials at high temperatures and in corresponding aggressive atmospheres.

Inasmuch as coatings during use are most frequently subjected to sudden heat changes, they should have a high thermal stability along with their insulating properties. An evaluation of the thermal impact resistance and the heat protecting properties of some nonmetallic coatings in an oxidizing atmosphere under conditions of intensive nonstationary thermal loading was made on a test stand with an elliptical heating device. Heat was produced by focused radiant energy, cooling by an air-water mixture vortex. The samples consisted of St. 3 steel cylinders, 5 mm diameter and 20 mm high, coated with aluminum oxide.

It was determined that in the substrate-coating combination the resistance of the coating to sudden heat changes was low. This apparently

was due to the fact that the thermal expansion coefficient of the metallic substrate is much higher than that of the coating, and also because the adhesive binder becomes weakened by the sudden heat changes. All of the failed samples had cracks which were oriented along the generatrix. At 1500-1600°K due to metal oxidation, the coating lost its bond with the substrate, cracked and crumbled.

The heat protecting properties of some coatings were tested on molybdenum. Samples, 5 mm diameter and 20 mm high, had three different types of coatings (Fig. 110): aluminum oxide (solid line), silicon (dotted line) and boron (dot-and-dash line). Samples were heated to 1900°K. Curves of the surface temperature growth and differences in the temperature of the surface and core show that the best coating for heat protection is aluminum oxide.

1170

Samples made of molybdenum alloy TsM-5 with bilayer protective coatings were tensile tested in an air oxidizing atmosphere. The first layer of the coating, directly applied onto the substrate by thermodiffusion, is a molybdenum disilicide  $MoSi_2$ , mixed with ammonium chloride powder; the second (outer) layer was of two types -- enamel (10%  $ZrO$  + 60%  $ZrO_2$  + 30% fusible glass) or hafnium dioxide  $HfO_2$ . The microstructures of these coatings is somewhat different due to the way in which they were applied and their subsequent heat treatment. After the enamel was applied it was baked at 1850-1900°K for two hours in a hydrogen atmosphere. During the baking process secondary diffusion processes occur between the molybdenum disilicide coating and TsM-5 alloy. This results in the formation of silicides with a lower silicon content, and a zone caused by the interaction of the molybdenum disilicide with the enamel forms on the boundary with the enamel. In addition, baking brings on recrystallization of the base TsM-5 material. When the

hafnium dioxide was applied, the sample was not heated and no significant secondary thermodiffusion processes were observed in it.

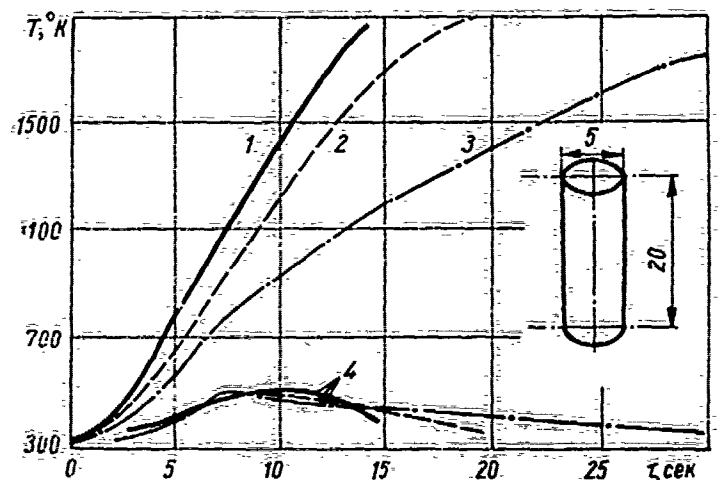


Fig. 110. Heat-reflecting properties of coatings applied to molybdenum:

- 1 - silicon;
- 2 - boron;
- 3 - aluminum oxide;
- 4 - temperature difference between sample surface and core.

The short-term strength on samples with these coatings was determined as follows after 300 sec of holding without load at 1900-2300°K: gradually bringing the sample closer to the focal plane of the solar furnace (samples were tested on a stand with a solar furnace described in section five, Chapter III), it was heated to the specified temperature (to avoid cracking the coating as a result of thermal impact the heating rate did not exceed 30 grad/sec), then it was held for 300 sec at a constant temperature without load. After the holding time elapsed the samples failed. Test results are shown on Fig. 111. Tensile strength was calculated on the starting section of the base material, measured before the coating was applied.

Preliminary data showed that samples coated with  $\text{MoSi}_2 + \text{HfO}_2$  had a higher heat resistance, therefore they were tested at 2100 and 2300°K. At these temperatures and 300 sec holding time, the coatings remained unchanged, sample strength changed very slightly and remained at a high level.

/171

Samples coated with  $\text{MoSi}_2 + \text{enamel}$  at 1900-2200°K had a much lower tensile strength. Increasing the testing temperature from 1900 to 2200°K at the same holding time to failure (300 sec) greatly lowers its strength. This is attributed to the effect of high temperature baking during the application of enamel (the interaction of the coating layers between themselves and the base material, its recrystallization and so forth). Also, after baking, the enamel has much lower heat insulating qualities than the sprayed-on hafnium dioxide, thus the enamel coating to a lesser degree prevents heat-through of the substrate material.

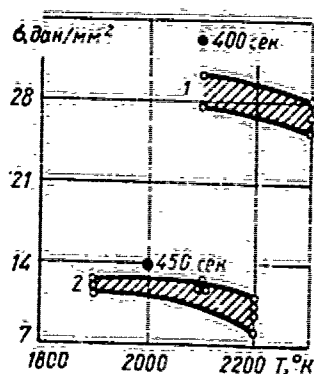


Fig. 111. Temperature dependence of tensile strength of coated TsM-5 alloy samples after holding 300 seconds.

- 1 - samples coated with  $\text{MoSi}_2 + \text{HfO}_2$ ;
- 2 - samples coated with  $\text{MoSi}_2 + \text{enamel}$ .

Tests showed that sample strength depends on the thickness of the protective coating. The results obtained at 2300°K and 300 sec holding time show that the strength drops greatly when the thickness of the  $\text{MoSi}_2 + \text{HfO}_2$  coating is decreased from 0.35 to 0.15 mm.

From the standpoint of gas permeability the thickness of the applied coatings is also important, inasmuch as tests were conducted in an oxidizing atmosphere. Visual examination of the samples during testing and after their failure showed the presence of air oxygen diffusion through the enamel coating; the samples "fume" due to the precipitation of gaseous oxidation products of the base material, and in individual samples an annular gap was detected between the enamel and the base after testing. A similar phenomenon was not observed on the samples coated with hafnium dioxide.

A comparison of the durability of the coatings made during thermal impact is quite interesting. To do this, samples were placed in the focal plane, shielded with a screen, of a solar furnace. Then the shielding screen was momentarily removed and a heat radiation of approximately  $10,500 \text{ kvt/m}^2$  fell on the sample. The enamel almost immediately cracked across the entire heated surface; the coating of hafnium dioxide, as a rule, had a higher thermal stability under these conditions.

The plastic properties of enamel are also worse than those of hafnium dioxide. Transverse cracks and spalls, forming as result of the different plasticity of the enamel and TSM-5 alloy, were very evident on the enamel samples after testing. This was not observed on the samples with the sprayed-on hafnium dioxide.

172 Because under actual conditions pieces with heat insulating coatings are subjected to mechanical loads, the effect of stress state on corrosion failure and strength of coated samples was determined. Fig. 112 shows the relationship of strength to the previously applied tensile load level for samples of TSM-5 alloy coated with  $\text{MoSi}_2 + \text{HfO}_2$  at 2100 and 2300°K. The experiment was conducted according to the method described above. However before heating, the sample was subjected to tensile forces, which were then

automatically maintained at a steady rate for 300 sec using a load stabilizing device described in paragraph five, Chapter III.

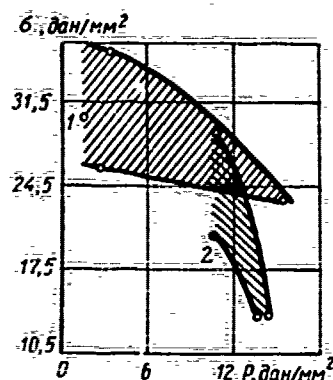


Fig. 112. Tensile strength of preheated TsM-5 alloy samples coated with  $\text{MoSi}_2 + \text{HfO}_2$ :

- 1 = at 2100°K;
- 2 = at 2300°K.

Test results indicate that prior loading of samples at 2100°K up to 50% of short-term failing load, produces no significant stress relief. When testing temperature is increased to 2300°K, an increased sensitivity to defects in the material is noted in the loaded sample. However in qualitative samples the failing load after 300 sec remained sufficiently high, which reflects the large strength reserve of the structural elements which have the described coating.

It is necessary to note the large scattering of experimental data, which apparently is due to the heterogeneity of the structure of the cold-worked TsM-5 alloy, as well as the different coating thickness, which has a great effect on the strength of the samples. In addition, TsM-5 alloy is susceptible to dispersion hardening due to carbide formation, which in turn, is related to many factors and therefore was reflected variously on different samples. This can be explained by the observed increase in strength in samples coated with  $\text{SiO}_2 + \text{enamel}$  at testing temperature 2000°K for 450 sec and coated with  $\text{MoSi}_2 + \text{HfO}_2$  at 2100°K for 400 sec (see Fig. 111). Apparently the

recrystallized structure of the samples after the enamel is baked has a lesser strengthening effect than the deformed structure coated with  $\text{MoSi}_2 + \text{HfO}_2$ .

Thus, tests indicated that heat protected coatings comprised of a thermodiffusion layer of  $\text{MoSi}_2$  and a sprayed-on hafnium dioxide are more effective and reliable than a bilayer coating of  $\text{MoSi}_2$  and enamel.

1. Alfrey T. Mekhanicheskiye svoystva vysokopolimérov. ("Mechanical properties of high polymers"). I.L. M., 1952.
2. Bartenev G.M. Stroyeniye i mekhanicheskiye svoystva neorganicheskikh stekol ("Structure and mechanical properties of inorganic glasses"). "STROITEL", M., 1966.
3. Bartenev G.M., Kotorina L.I. -- DAN AN SSSR, 1963.
4. Baum V.A. -- In the book: Solnechniye pechi ("Solar furnaces") 1960.
5. Byelozérov A.B., Malakhov N.A. -- In the book: Trudy TsAGI. ("Proceedings of the Central Institute of Aerodynamics") ONTI TsAGI, 9, 1966.
6. Byeloiyan A.F. et al. -- Mekhanizatsiya i avtomatizatsiya upravleniya. IIL, Kiev, 1966, 4.
7. Byeloiyan A.F., Gashchenko A.G., Isakhanov G.V. -- Mekhanizatsiya i avtomatizatsiya upravleniya. IIL, Kiev, 1966, 6.
8. Eyeno et. al. -- Sinteticheskiye i vysokomolekulyarnye materialy, VINITI, 1957, 33.
9. Eyerezhnoy A.I., sitalis and photositalis. "Mashinostroveniye", M., 1966.
10. Bol'shin M. Yu., Likhtman V.I. -- In the book: Issledovaniye po zharoprochnym splavam ("Investigation of heat-resistant alloys"), 8. Publ. AN SSSR, M., 1962.
11. Birger I.A. Rukovodstvo dlya konstruktorov po raschetu na prochnost' gazoturbinnogo dvigatelya ("Guide for designers on gas turbine engine strength calculation"). Oborongiz, M., 1956.
12. Bogorad M.L., Loshkarev M.A., Lipov I.G. -- Plasticheskiye massy, 1963, 8.
13. Bogorad M.L., Loshkarev M.A. -- In the book: Teploviye napryazheniya v elementakh konstruktsiy ("Thermal stresses in structural elements"), 5, "Naukova dumka", Kiev, 1965.
14. Voli B., Weiner, J. Teoriya temperaturnykh napryazheniy ("Theory of temperature stresses") "Mir", M., 1964.
15. Bronstein I.N., Semendyaev K.A., Spravochnik po matematike ("Mathematics handbook"), "Nauka", M., 1967.

16. Vishnevskiy G.E., Cand. Dissert. Engineering Institute, M., 1963.
17. Voloshchenko A.P. -- In the book: Termoprochnost' materialov i konstruktivnykh elementov ("Thermal strength of materials and structural elements"). "Naukova dumka", Kiev, 1967.
18. Geitvud B.E. Temperaturnye napryazheniya ("Temperature stresses"). IL, M., 1959.
19. Gogotsi G.A., Tret'yachenko G.N. -- In the book: Termoprochnost' materialov i konstruktivnykh elementov ("Thermal strength of materials and structural elements"). "Naukova dumka", Kiev, 1965.
20. Gogotsi G.A., Iankin Yu.N. -- In the book: Termoprochnost' materialov i konstruktivnykh elementov ("Thermal strength of materials and structural elements"). "Naukova dumka", Kiev, 1967.
21. Gogotsi G.H. -- Cand. Dissert. IPM AN UkrSSR, Kiev, 1966.
22. Grekov D.I. -- Energomashinostroyeniye, 1961, 10.
23. Gurevich V.Z. Elektricheskiye infrakrasnyye izluchateli ("Electrical infrared radiators"). GEM, M., 1963.
24. Gumenyuk V.S., Kritsuk A.A., Lositskiy V.I. -- In the book: Termoprochnost' materialov i konstruktivnykh elementov ("Thermal strength of materials and structural elements"). "Naukova dumka", Kiev, 1967.
25. Gukhman, A.A. Vvedeniye v teoriyu podobiya ("Introduction to the similarity theory"). "Vysshaya shkola", M., 1963.
26. Dantsova E.P. et al. -- Plasticheskiye massy, 1964, 4.
27. Demishev G.K. -- Steklo. GIS Bulletin, 1964, 4, 1.
28. Demishev G.K. -- Steklo. GIS Bulletin, 1962, 4, 1.
29. Drakin I.I. Aerodinamicheskii i luchistiy nagrev v polete ("Aerodynamic and radiant heat in flight"). Oborongiz, M., 1961.
30. Dudarov I.G., Poluboyarinov D.N., -- Ogneupory, 1963, 11.
31. Efimova V.S. et al. -- In the book: Metody ispytaniya polimernykh materialov ("Methods for testing polymeric materials"). ONTI VIAM, M., 1963.
32. Zhurkov S.N. -- ZhIF, 1955, 1.
33. Zalmang G. Fiziko-khimicheskiye osnovy keramiki ("Physico-chemical bases of ceramics"). 1959.

/174

34. Isakhanov G.V., Dzhyuba V.S. -- Fiziko-khimicheskaya mekhanika materialov ("Physico-chemical mechanics of materials"). 1968, 2.
35. Isakhanov G.V., Lyashenko B.A. Authors' Cert. No. 165921, 1965.
36. Isakhanov G.V., Lyashenko B.A. -- In the book: Voprosy vysokotemperaturnoy prochnosti v mashinostroyenii ("Problems of high-temperature strength in machine building"). Publ. AN UkSSR, Kiev, 1963.
37. Isakhanov G.V., Lyashenko B.A. Peredovoy nauchno-tekhnicheskiy i proizvodstvenny opyt ("Advanced scientific-technical and production experience"). GOSINTI, M., 1965.
38. Isakhanov G.V., Lyashenko B.A. -- Poroshkovaya metallurgiya, 1965, 9.
39. Isakhanov G.V., Lyashenko B.A., Sterniyak V.A. -- Mashinostroyeniye, ITI, Kiev, 1965, 1.
40. Issledovaniye pri vysokikh temperaturakh ("Investigation high temperatures"). IL, M., 1962.
41. Kaynarskiy I.E. Dinas ("Dinas brick"). Metallurgizdat, M., 1961.
42. Kargin V.A. -- Plasticheskiye massy, 1961, 1.
43. Kargin V.A., Slonimskiy G.L. Kratkiye ochërki po fiziko-khimii polimerov ("A brief outline on the physical chemistry of polymers"). Publ. MGU, M., 1960.
44. Keller E.K. Termomekhanicheskiye svoystva alyumosilikatnykh ogneporov ("Thermo-mechanical properties of aluminosilicate refractories"). Metallurgizdat, M., 1949.
45. Kingery W.D. -- In the book: Izmereniya pri vysokikh temperaturakh ("High-temperature measurements"). IL, M., 1963.
46. Kingery W.D. Vvedeniye v keramiku ("Introduction to Ceramics"). IL, M., 1964.
47. Kirpichev M.V., Konakov P.K. Matematicheskiye osnovy teorii podobnaya ("Mathematical basis of the similarity theory"). Gosenergoizdat, M., 1949.
48. Kiselev E.A. Stekloplastiki ("Glass-fiber-reinforced plastics"). Goskhimizdat, M., 1961.
49. Kiselev E.A., Gribova A.M. -- Plasticheskiye massy, 1962, 5
50. Klyavin O.V. -- Zavodskaya laboratoriya, 1963, 4.

51. Kortén Kh. T. Razrusheniye armirovannykh plastikov ("Breakage of reinforced plastics"). "Khimiya", M., 1967.
52. Kostanyan K.A., Saakyan M.S. -- Steklo i keramika, 1960, 8.
53. Koshelev P.F., Makhmutov I.M., Stepanychev E.I. -- Plasticheskiye massy, 1963, 4.
54. Kravchuk L.V. -- Cand. Dissert. IPM AN UkrSSR, Kiev, 1963.
55. Zuzimin M.A. Raschet i konstruirovaniye bezynertsionnykh pechey ("Design and construction of inertia-free furnaces"). M. = L., 1961.
56. Kukolov G.V., Nemets I.I., Khonyakov M.T. -- Steklo i keramika, 1962, 2.
57. Kukolov G.V., Nemets I.I. -- Ogneupory, 1964, 5.
58. Lozinskiy M.G., Vishnevskiy G.E., Pavlov A.I. -- In the book: Termoprochnost' materialov i konstruktivnykh elementov ("Thermal strength of materials and structural elements"). "Naukova dumka", Kiev, 1965.
59. Lozinskiy M.G., Vishnevskiy G.E. -- IMASH-11 test stand for studying mechanical properties of sheet materials during one-sided heating. GOSINTI, M., 1963.
60. Lozinskiy M.G. et al. -- In the book: Termoprochnost' materialov i konstruktivnykh elementov ("Thermal strength of materials and structural elements"). "Naukova dumka", Kiev, 1967.
61. Lozinskiy M.G., Vishnevskiy G.E. -- Plasticheskiye massy, 1964, 4.
62. Lykov A.V. Teoriya teploprovodnosti ("Theory of heat conductivity"). "Vysshaya shkolov", M., 1957.
63. Lyashenko B.A. Cand. Dissert. IPM AN UkrSSR, Kiev, 1963.
64. Lyashenko B.A., Isakhanov G.V. -- Zavodskaya laboratoriya, 1965, 10.
65. MacMillan P.U. Steklokeramika ("Glass ceramics"), "Mir", M., 1967.
66. Maliniu N.M. -- DAN AN SSSR, ONT, 1954, 4.
67. Minyailo A.A., Isakhanov G.V., -- In the book: Termoprochnost' materialov i konstruktivnykh elementov ("Thermal strength of materials and structural elements"). "Naukova dumka", Kiev, 1967.
68. Mishcheuko A.M., Tsyplakov G.G. -- In the book: Armirovaniye stekloplastiki ("Reinforced glass plastics"). Publ. LMI, L., 1966.
69. Molchanov E.I., Butyakov V.N. -- In the book: Termoprochnost' materialov i konstruktivnykh elementov ("Thermal strength of materials and structural elements"). "Naukova dumka", Kiev, 1967.

70. Vorh Dzh. -- In the book: Mekhanicheskiye svoystva novykh materialov ("Mechanical properties of new materials"). "Mir", M., 1966.
71. Vorozov E.M., Fridman Ya.B. -- In the book: Prochnost' i deformatsiya v neravnomernykh temperaturnykh pol'yakh ("Strength and deformation in non-uniform temperature fields"). Gosatomizdat, M., 1962.
72. Nikulin V.N., Skurikhin V.G. -- Avtomaticheskaya svarka, 1960, 10.
73. Nikulin V.N., Kvachev V.G. -- Avtomatika i priborostroyeniye, 1963, 2.
74. Nikulin V.N., Kvachev V.G. -- Avtomaticheskaya svarka, 1963, 5.
75. Ogibalov P.M., Lomakin V.A. -- In the book: Inzhenerny sbornik ("Engineering handbook"), Publ. MGU, 30, 1960.
76. Ogibalov P.M., Suvorova Yu.V. -- Mekhanika armirovannykh plastikov ("Mechanics of reinforced plastics"), Publ. MGU, M., 1965.
77. Panarin A.P., -- Ogneupory, 1964, 4.
78. Parfenov K.V., Romanenkov I.G. -- Stroitelnye materialy, 1962, 3.
79. Panshin B.I., Vishnevskiy G.E., Plasticheskiye massy, 1961, 10.
80. Panshin B.I., Vishnevskiy G.E., Plasticheskiye massy, 1961, 3.
81. Panshin B.I., Vishnevskiy G.E., Plasticheskiye massy, 1963, 3.
82. Panshin B.I. -- In the book: Metody ispytaniya polimernykh materialov ("Methods for testing polymeric materials"). ONTI VIAM, M., 1963.
83. Peyches I. -- In the book: Problemy vysokikh temperatur v aviatsionnykh konstruktsiyakh ("High-temperature problems in aviation structures"). IL, M., 1961.
84. Pines E.Ya. -- ZhTF, 1938, 8, 24.
85. Pisarenko G.S. et al. -- In the book: Prochnost' materialov pri vysokikh temperaturakh ("Strength of materials at high temperatures"). "Naukova dumka", Kiev, 1966.
86. Pisarenko G.S., Lyashenko B.A., Isakhanov G.V. -- In the book: Termoprochnost' materialov i konstruktivnykh elementov ("Thermal strength of materials and structural elements"). "Naukova dumka", Kiev, 1965.
87. Polucheniye i issledovaniye vysokotemperaturnoy plazmy ("Production and study of high-temperature plasma"). IL, M., 1962.

88. Ponomarev S.D. et al. -- Raschetny na prochnost' v mashinostroyeni ("Strength calculations in machine building"). Mashgiz, M., 1956.
89. Rabinovich A.L., Shgarkov M., Dmitrieva E.I. -- In the book: Issledovaniye po mekhanike i prikladnoy matematike; ("Study of mechanics and applied mathematics"). Publ. MFTI., M., 1958.
90. Rakovskiy V.A. -- Vvedeniye v fizicheskuyu khimiyu ("Introduction to physical chemistry"). Gostekhizdat, M., 1958.
91. Rzhantsyn A.R. -- Teoriya polzuchesti ("Creep theory"). Stroyizdat, M., 1968.
92. Samolétostroyeniye (express - information VINITI), 1957, 13.
93. Sedov L.I. -- Metody podobiya i razmernosti v mekhanike ("Similarity and dissimilarity methods in engineering"). "Nauka", M., 1965.
94. Serebryakov M.E. Vnutrennyaya ballistika ("Internal ballistics"). Oborongiz, M., 1962.
95. Skurikhin V.I., Nikulin V.M., Drymalyk Ya.I., -- In the book: Voprosy vychislitel'noy tekhniki ("Calculating techniques"). Gostekhizdat UkrSSR, Kiev, 1961.
96. Smirovich et al. -- Sudostroyeniye, 1965, 6.
97. Sobolevskiy M.V., Bodrova V.V. -- Aviatsionnaya promyshlennost'. 1957, 2.
98. Somov A.I., Cherny C.V. -- In the book: Termoprochnost' materialov i konstruktivnykh elementov ("Thermal strength of materials and structural elements"). "Naukova dumka", Kiev, 1967.
- \*  
100. Strelyayev V.S. -- Cand. Dissert, Engineering Institute, M., 1963.
101. Tarnopol'skiy Yu.M., Rose A.V. Mekhanika polimerov, 1965, 2.
102. Tarnopol'skiy Yu.M., Rose A.V. Mekhanika polimerov, 1965, 5.
103. Tarnopol'skiy Yu.M., Rose A.V. Mekhanika polimerov, 1966, 4.
104. Tarnopol'skiy Yu.M., Skudra A.M. Konstruktivnyaya prochnost' i deformativnost' stekloplastikov ("Structural strength and deformability of glass-fiber-reinforced plastics"). "Zinatne", Riga, 1966.
105. Timoshenko S.P. Soprotivleniye materialov ("Material resistance"). "Nauka", M., 1.
- /176  
106. Tikhonov N.I. Zavodskaya laboratoriya, 1962, 9.
107. Tret'yachenko G.N. Poroshkovaya metallurgiya, 1963, 1.
- \*99. Steynberg, M. A., Kerfut, Kh. P. V kh.: Investigation of high temperatures. "Nauka" M., 1967.

108. Tret'yachenko G.N. -- In the book: Termoprochnost' materialov i konstruktivnykh elementov ("Thermal strength of materials and structural elements"). "Naukova dumka", Kiev, 1967.
109. Troshchenko V.T. Prorashkovaya metallurgiya, 1963, 3.
110. Troshchenko V.T. Poroshkovaya metallurgiya, 1964, 6.
111. Tynnyy A.M., Soshko A.I. Fiziko-khimicheskaya mekhanika materialov ("Physics-chemical engineering of materials"). 1965, 3.
112. White, G.K. Ekspèrimental'naya tekhnika v fizike nizkikh temperatur ("Experimental techniques in low-temperature physics"). IL, M., 1961.
113. Finkelberg V., Mekker T. Elektricheskiye dugi i termicheskaya plazma ("Electrical arcs and thermal plasma"). IL, M., 1961.
114. Hoff H. -- In the book: Problemy vysokikh temperatur aviatsionnykh konstruktivnykh ("High-temperature problems in aviation structures"). IL, M., 1961.
115. Khu L., Markin J. -- In the book: Mekhanika ("Engineering"), IL, M., 1956.
116. Tsyplakov O.G. -- In the book: Armirovannyye stekloplastiki ("Glass-fiber-reinforced plastics"). Publ. LMI, L., 1966.
117. Tsyplakov O.G. Plasticheskiye massy, 1964, 3.
118. Chistoserdov V.G., Soboleva I.A. Optikomekhanicheskaya promyshlennost'. 1962, 9.
119. Shvidenko V.I. Cand. Dissert. IPM AN UkrSSR, Kiev, 1966.
120. Shvidenko V.I., Lyashenko B.A. Zavodskaya laboratoriya, 1966, 5.
121. Shvidenko V.I., Lyashenko B.A., Isakhanov G.V. -- In the book: Termoprochnost' materialov i konstruktivnykh elementov ("Thermal strength of materials and structural elements"). "Naukova dumka", Kiev, 1967.
122. Yakovlev G.A. -- In the book: Teplovyé napryazheniya v elementakh konstruktivnykh, 4. ("Heat stresses in structural elements"). "Naukova dumka", Kiev, 1964.
123. Yakovlev G.A. -- In the book: Termoprochnost' materialov i konstruktivnykh elementov ("Thermal strength of materials and structural elements"). "Naukova dumka", Kiev, 1967.
124. Borel -- J. Soc Glass Techn., 1950, 34, 160.
125. Brearsley W., Holloway D. Phys. Chem Glasses, 1964, 4.

126. Chamberlain D.W. Adv. Cryog. Eng., 1964, 9.
127. Coble R.L., Kingery W.D. J. Am. Cer. Soc., 1955, 38, 1.
128. Farber I. Missile Aerophysics, Pamphlet, 1957.
129. Goethert B.H. ARS J. 1962, 32, 6.
130. Hargreaves F. Trans. Brit. Cer. Soc., 1958, 5.
131. Hinz W., Baiburt Z. Silikattechn., 1960, 11, 10.
132. Jaffe L.D., Rittenhouse I.B. ARS J. 1962, 32, 3.
133. Jakob M. Heat Transfer, 1949, 1.
134. Jones G., Turner W.I. Soc. Glass Technol., 1942, 26, 35.
135. Kingery W.D. Property Measurements at high Temp., 1957.
136. Kingery W.D. J. Am. Cer. Soc., 1958, 38, 1.
137. McAbee E., Ohmura M. Proc of 16th Annual SPI Conference Reinforced Plastics Divis, 1961.
138. Outwater I.O. ASME Papers, 1956, 56 - A = 201.
139. Parrat N.I. Rubber and Plastics, 1960.
140. Porter R.W., Mitchell M.W., Drummond F.C. Le Vide, 1965, 20, 115.
141. Ritter I., Cooper A. Phys. Chem. Glasses, 1963, 4, 73.
142. Scala, Gilbert ARS J. 1962, 6.
143. Schmitz G.K. Progress Report, 1962, 4.
144. Schwartz E. J. Am. Cer. Soc., 1952, 12.
145. Smekal A.I. Soc. Glass Technol. 1936, 20.
146. Smekal A.I. Glasstechnol. 1950, 23, 57.
147. Stanworth I.E. Phys. properties of Glass, 1940.
148. Wende A., Moebes W., Marten H. Glasfaserverstärkte Plaste, 1963.
149. White I. Trans. Brit. Cer. Soc., 1958, 10.
150. Winkelmann A., Schott O. Phys. Chem., 1894, 51.

## Table of Contents

Foreword .....	3
Chapter I. Mechanical properties of nonmetallic materials during heating and loading .....	5
1. Physical-mechanical properties of structural nonmetallic materials .....	5
2. Structural characteristics of reinforced plastics .....	10
3. Strength-temperature dependence of reinforced plastics .....	16
4. High-temperature strength of glass and silalls .....	22
Chapter II. Characteristics of thermomechanically testing nonmetallic materials during non-uniform heating .....	27
1. Testing during one-sided heating .....	27
2. Testing for thermal stability .....	38
Chapter III. Methods and set-ups for studying the supporting capacity of nonmetallic materials and structural elements during intense one-sided heating .....	45
1. Methods for intense one-sided heating of nonmetallic materials .....	45
2. Set-up for mechanically testing nonmetallic materials at high temperatures .....	54
3. Set-ups for determining the supporting capacity of reinforced plastics during one-sided heating by electrical resistance .....	61
4. Set-ups for mechanically testing nonmetallic materials during one-sided heating in reverberatory furnaces .....	73
5. Set-ups for determining the supporting capacity of nonmetallic materials under conditions of combination cooling and one-sided heating .....	84
6. Set-up for determining the supporting capacity of structural elements made of nonmetallic materials under a complex stress state and one-sided heating .....	88

Chapter IV.	Mechanism of weakening in structural glass-fiber-reinforced plastics in one-sided heating under first order boundary conditions .....	95
1.	Strength and deformability of FN, SK-9F, KAST-V and VFT-S structural fiberglass laminates .....	95
2.	Life of AG-4S and EF-S glass-fiber-reinforced plastics during programmed heating and cooling .....	102
Chapter V.	Supporting capacity of glass-fiber-reinforced plastics in intense one-sided heating under second order boundary conditions .....	108
1.	Method for determining "instantaneous" supporting capacity of sample during intense, one-sided heating .....	108
2.	Supporting capacity of glass-fiber-reinforced plastics under bending conditions .....	113
3.	Influence of external medium pressure on supporting capacity of glass-fiber-reinforced plastics during intense one-sided heating .....	117
4.	Influence of pre-cooling on supporting capacity of glass-fiber-reinforced plastics during intense one-sided heating .....	127
5.	Bending of a reinforced plastic bar under one-sided heating .....	129
6.	Evaluation of the supporting capacity of reinforced plastics and structural elements during unsteady one-sided heating .....	136
Chapter VI.	Thermal stability of refractory materials .....	145
1.	Set-up for testing ring and small cylindrical samples for thermal stability .....	147
2.	Thermal stability of ring and small cylindrical samples .....	158
3.	Thermal stability and heat-protecting properties of some nonmetallic coatings .....	168
References	.....	173

DISTRIBUTION LIST

DISTRIBUTION DIRECT TO RECIPIENT

<u>ORGANIZATION</u>	<u>MICROFICHE</u>	<u>ORGANIZATION</u>	<u>MICROFICHE</u>
A205 DMATC	1	E053 AF/INAKA	1
A210 DMAAC	2	E017 AF/RDXTR-W	1
B344 DIA/RDS-3C	9	E403 AFSC/INA	1
C043 USAMIIA	1	E404 AEDC	1
C509 BALLISTIC RES LABS	1	E408 AFWL	1
C510 AIR MOBILITY R&D	1	E410 ADTC	1
C513 PICATINNY ARSENAL	1	FTD	
C535 AVIATION SYS COMD	1	CCN	1
C591 FSTC	5	ASD/FTD/NIIS	3
C619 MIA REDSTONE	1	NIA/PHS	1
D008 NISC	1	NIIS	2
H300 USAICE (USAREUR)	1		
P005 DOE	1		
P050 CIA/CRS/ADD/SD	2		
NAVORDSTA (50L)	1		
NASA/KSI	1		
AFIT/LD	1		
I.L.L./Code I.-389	1		
NSA/1213/TDL	2		

FTD-ID(RS)T-0225-79